



• U • C •

FCTUC FACULDADE DE CIÊNCIAS  
E TECNOLOGIA  
UNIVERSIDADE DE COIMBRA

DEPARTAMENTO DE  
ENGENHARIA MECÂNICA

# **Evolution of the vibrational behaviour of a guitar subjected to localized vibratory excitation**

Submitted in Partial Fulfilment of the Requirements for the Degree of Master in  
Mechanical Engineering in the speciality of Production and Project

## **Evolução do comportamento dinâmico de uma guitarra submetida a tratamento vibratório localizado**

**Author**

**João Pedro de Aragão Alegria Oliveira**

**Advisors**

**Amílcar Lopes Ramalho**

**Vincent Georges Mickael Debut**

**Jury**

**President** Professor Doutor Fernando Jorge Ventura Antunes  
Professor Auxiliar da Universidade de Coimbra

**Vowels** Professor Doutor Amílcar Lopes Ramalho  
Professor Associado c/ Agregação da Universidade de Coimbra  
Professor Doutor José Leandro Simões de Andrade Campos  
Professor Associado da Universidade de Coimbra

**Institutional Collaboration with FCSH/NOVA**

---



**Faculdade de Ciências Sociais e Humanas da  
Universidade Nova de Lisboa**

**Coimbra, September, 2018**



“Without music, life would be a mistake...  
I would only believe in a God who knew how to dance.”

Friedrich Nietzsche, in *Twilight of the Idols*, 1889

Aos meus pais, à Sara e à FAN-Farra Académica de Coimbra.



## Acknowledgements

O trabalho que aqui se apresenta só foi possível graças à colaboração e apoio de algumas pessoas, às quais não posso deixar de prestar o meu reconhecimento. Agradeço ao Professor Doutor Amílcar Ramalho pela disponibilidade de me deixar embarcar neste projeto. Agradeço ao Professor Doutor Vincent Debut por todo o apoio, paciência, rigor científico, amizade e sabedoria partilhada. Agradeço também ao Professor Doutor Paulo Vaz de Carvalho pela gentileza de nos ceder uma das suas guitarras e por se disponibilizar para a tocar, enchendo-a de vida e dados necessários ao nosso problema. Obrigado Isaac pela amizade, companheirismo e disponibilidade para ajudar em tudo o que fosse preciso. Agradeço ao INET e à FCSH da Universidade Nova de Lisboa por me terem acolhido e providenciado com tudo o que precisava. Por fim agradeço o apoio e interesse do Professor Doutor José Antunes no projeto e pela sua ajuda no desenvolvimento da parte experimental, imprescindível ao nosso estudo.



## Abstract

It is well accepted that musicians who play string instruments, taking the example of violins and guitars, believe that the sound quality of their instruments improves with age and/or regular practice. This motivated the appearance of commercially available products that promise to improve instrument sound through the exposure to continuous forced vibrations. In search of scientific evidence on the effect of playing-induced vibrations on tone quality, we develop a mechanical set-up intended to reproduce the mechanical vibrations undergone by guitars when played by musicians, and then apply a specific vibration treatment on a test guitar. Solving an inverse problem, we successfully identify the drive signal to be applied on the guitar in order to accurately reproduce acceleration signals measured on the guitar body when played by a professional guitarist. Using the developed set-up, the test guitar is then submitted to a continuous daily treatment under controlled conditions of temperature and humidity. Experimental modal analysis of the guitar is then regularly performed at different stages of the treatment, thus allowing to study the evolution of the vibrational properties of the instrument during the treatment. The intention is then to prove or disprove the effect that these vibrations could influence the dynamical behaviour of the instrument, and to allow in the future, the development of further studies to evaluate the effects of the total vibration time, the changes in temperature and relative humidity, among others.

**Keywords** Experimental Modal Analysis, Inverse Problem, Artificial Playing, Vibration Treatment, Music Acoustics.



## Resumo

É amplamente reconhecido que músicos que tocam instrumentos de corda, tomando o exemplo do violino e da guitarra, acreditam que a qualidade de som dos seus instrumentos melhora com a sua idade e/ou uso constante. Isto justificou o surgimento de aparelhos comerciais que prometem melhorar a qualidade dos instrumentos através de vibrações contínuas forçadas. Na procura de evidência científica sobre o efeito das vibrações, induzidas quando o instrumento é tocado, na qualidade do seu timbre, desenvolvemos um *set-up* mecânico com o intuito de reproduzir as vibrações mecânicas que a que as guitarras estão sujeitadas quando são tocadas e depois aplicar um tratamento vibratório numa guitarra de teste. Resolvendo um problema inverso, identificamos com sucesso o sinal a ser aplicado na guitarra de forma a reproduzir fielmente os sinais de aceleração medidos no corpo da guitarra quando esta foi tocada por um guitarrista profissional. A guitarra é então submetida a um tratamento contínuo diário com a aplicação destas mesmas vibrações, num ambiente de temperatura e humidade controlados. Em diferentes fases do tratamento, efetuamos uma análise modal experimental da guitarra na gama das baixas frequências, permitindo acompanhar a evolução das propriedades vibratórias do instrumento com o tempo de excitação. A intenção será de provar ou negar o efeito que estas vibrações possuem no comportamento dinâmico do instrumento e que o tratamento vibratório desenvolvido possa ser utilizado em futuros estudos para avaliar melhor os efeitos do tempo total de vibração, as variações de temperatura e humidade relativa, entre outros.

**Palavras-chave:** Análise Modal Experimental, Problema inverso, Tocar artificial, Tratamento vibratório, Acústica Musical.



---

## Contents

|   |           |
|---|-----------|
| List of figures .....   | ix        |
| List of tables .....  | xi        |
| Symbology and acronyms .....                                  | xiii      |
| Symbology.....  | xiii      |
| Acronyms .....  | xiii      |
| <b>1. Introduction .....</b>                                  | <b>1</b>  |
| <b>2. Project Scoping and Literature Review .....</b>         | <b>3</b>  |
| 2.1. Project scope .....                                      | 3         |
| 2.2. Brief history of stringed instruments .....              | 3         |
| 2.3. Mechanics of stringed instruments .....                  | 4         |
| 2.4. Dynamic and modal response of classical guitars .....    | 7         |
| 2.5. Concept of sound quality and instrument ageing.....      | 8         |
| 2.6. Previous related studies .....                           | 11        |
| <b>3. Experimental Modal Analysis .....</b>                   | <b>19</b> |
| 3.1. Industrial applications.....                             | 19        |
| 3.2. Applications in Music Acoustics .....                    | 20        |
| 3.3. Modal identification technique .....                     | 22        |
| 3.3.1. Eigensystem Realization Algorithm's formulation.....   | 23        |
| 3.3.2. Experimental Set-up .....                              | 27        |
| <b>4. Vibration Treatment .....</b>                           | <b>37</b> |
| 4.1. Inverse Problem .....                                    | 37        |
| 4.2. Experimental Set-up .....                                | 41        |
| 4.2.1. Recording acceleration .....                           | 41        |
| 4.2.2. Measuring transfer-function and vibration set-up ..... | 42        |
| 4.3. Results.....   | 44        |
| <b>5. Experimental Protocol .....</b>                         | <b>47</b> |
| <b>6. Treatment and Results .....</b>                         | <b>49</b> |
| 6.1. Applied treatment.....                                   | 49        |
| 6.2. Preliminary Results.....                                 | 49        |
| <b>7. Conclusions .....</b>                                   | <b>53</b> |
| Bibliography .....  | 55        |



## List of figures

|   |    |
|---|----|
| Figure 1 Early forms of string instruments (Viridung, 1511).....  | 4  |
| Figure 2 Early Romantic guitar (ca.1830, Paris).....  | 4  |
| Figure 3 Examples of symmetrical and asymmetrical top plate patterns: (a) Smallman (Australia); (b) Fleta (Spain); (c) Eban (USA) (Rossing, 2010) .....                               | 5  |
| Figure 4 Classical guitar neck cross-section (Rossing, 2010).....   | 6  |
| Figure 5 Detailed anatomy of a classical guitar .....   | 6  |
| Figure 6 Top Plate, Back Plate and Air vibration modes (Rossing, 2010) .....  | 7  |
| Figure 7 Breathing modes of a freely supported Martin D-28 guitar in the low frequency region (Fletcher & Rossing, 1998).....   | 7  |
| Figure 8 First vibrational modes found in most classical guitars (Christensen, 1984) .....  | 8  |
| Figure 9 Frequency response function for a bad and good guitar (S. Šali & Kopač, 2000)..  | 9  |
| Figure 10 Sound pressure for excitation frequency of a cello after 4 years of playing (Hutchins, 1998).....   | 11 |
| Figure 11 Sound pressure for excitation frequency of a violin subjected to vibration tests (Hutchins, 1998).....  | 12 |
| Figure 12 Variation of the damping coefficient with forced vibrations (Hunt & Balsan, 1996).....  | 12 |
| Figure 13 Viscoelastic model (Akahoshi et al., 2005) .....  | 13 |
| Figure 14 Change of $E'$ and $\tan\delta$ in time (Akahoshi et al., 2005) .....   | 14 |
| Figure 15 Frequency response functions obtained for the guitar pairs (Clemens et al., 2014) .....   | 17 |
| Figure 16 Output of the guitar-top mounted accelerometer as function of time during a gentle strum from a strumming device and during vibration treatment (Clemens et al., 2014)..... | 18 |
| Figure 17 Analytical and experimental modal analysis of a building (Døssing, 1988a) ....  | 20 |
| Figure 18 Holographic interferograms of a classical guitar (Richardson & Roberts, 1985)   | 21 |
| Figure 19 Stability diagram (Brown et al., 1979).....   | 27 |
| Figure 20 Free-boundary guitar set-up .....   | 27 |
| Figure 21 Illustrative diagram of the experimental set-up for modal identification .....  | 28 |
| Figure 22 Effect of double hits (Døssing, 1988b) .....  | 29 |
| Figure 23 The tested guitar with the mesh of measurement points.....  | 30 |
| Figure 24 Experimentally obtained input impulse and FRF.....  | 31 |

|   |    |
|---|----|
| Figure 25 FRF with stability diagram .....  | 32 |
| Figure 26 Selection of the real modal parameters.....   | 32 |
| Figure 27 Comparison between the measured and identified impulse response and transfer function .....     | 33 |
| Figure 28 First mode shape of the guitar.....   | 34 |
| Figure 29 Second and third mode shapes.....   | 35 |
| Figure 30 Fourth identified mode shape .....  | 35 |
| Figure 31 Fifth identified mode shape .....   | 36 |
| Figure 32 Sixth identified mode shape.....  | 36 |
| Figure 33 Typical L-Curve (Hansen, 2000).....   | 40 |
| Figure 34 Professor Paulo Vaz de Carvalho recording of playing acceleration .....                         | 41 |
| Figure 35 Experimental set-up for determining the transfer function.....                                  | 42 |
| Figure 36 Experimental set-up for vibration treatment.....  | 43 |
| Figure 37 Detail of the shaker and accelerometer from the experimental-setup for vibration treatment..... | 44 |
| Figure 38 Plotted L-Curve.....  | 44 |
| Figure 39 Application of the critical level .....   | 45 |
| Figure 40 Measured acceleration and corresponding identified voltage.....                                 | 45 |
| Figure 41 Comparison between the original acceleration signal and the one reproduced..                    | 46 |
| Figure 42 Zoomed in comparison between original and reproduced acceleration .....                         | 46 |
| Figure 43 Transfer function comparison.....   | 50 |
| Figure 44 Transfer function comparison zoom on the 260Hz mode.....  | 50 |

---

## List of tables

|  |    |
|--|----|
| Table 1 Pearson's Correlations (Clemens et al., 2014) .....            | 17 |
| Table 2 Modal parameters before treatment.....                         | 33 |
| Table 3 Applied treatments.....  | 49 |
| Table 4 Evolution of modal identification parameters in point 154..... | 51 |
| Table 5 Evolution of modal identification parameters in point 130..... | 51 |



## Symbology and acronyms

### Symbology

$E$  – Young's modulus

$\mathcal{F}$  – Fourier transform

$H_i$  – Initial relative humidity

$H_f$  – Final relative humidity

$r$  – Pearson's correlation

$\tan\delta$  – Loss tangent

$T_i$  – Initial temperature

$T_f$  – Final temperature

$w_n$  – Modal frequency

$\zeta_n$  – Modal damping

$\varphi$  – Mode shape

$\lambda_n$  – Eigenvalues

### Acronyms

ERA – Eigensystem Realization Algorithm

FRF – Frequency Response Function

MDOF – Multiple-degree-of-freedom

MIMO – Multiple Input Multiple Output

SDOF – Single-degree-of-freedom

SIMO – Single Input Multiple Output

SISO – Single Input Single Output

SVD – Singular Value Decomposition



## 1. INTRODUCTION

The sound of stringed instruments comes from the combination of vibrating strings coupled with a resonant body. This body, that allows the radiation of sound, is a complex construction usually handcrafted by experienced artisans with empirical and traditional knowledge passed throughout hundreds of years of instrument making. The shaping, arrangement and material from which the vibrating components are made is of utmost importance to the quality of the vibration and sound of the instrument.

It is widely believed by professional musicians that the sound of instruments improves with age and/or regular playing (Akahoshi, Chen, & Obataya, 2005; Hunt & Balsan, 1996; Inta, Smith, & Wolfe, 2005; Obataya, 2017). Previous studies have reported mechanical measurable differences associated with the regular playing of violins (Hutchins, 1998) and with forced vibrations applied to wood (Akahoshi et al., 2005; Hunt & Balsan, 1996; Sobue & Okayasu, 1992), while playing and listening subjective tests have shown no statistically significant differences (Inta et al., 2005). Along with the desire to constantly improve instrument sound, commercially available products that promise to improve instrument sound through the exposure to continuous forced vibrations exist (Turner, 1997), to which a study has been made, apparently showing no significant differences in both subjective listening tests as well as in frequency response functions, when guitars are excited at a constant frequency (Clemens et al., 2014).

With this study it is intended to study the “playing-in” of a classical guitar making use of ageing/playing-in through a wideband forced vibration that can simulate a long term and intense regular playing. Prior, during and post this treatment, experimental modal analysis will be used to identify changes in the modal parameters (natural frequencies, damping factors and shape modes) proving or disproving that the instrument vibrational behaviour has been altered.



## 2. PROJECT SCOPING AND LITERATURE REVIEW

### 2.1. Project scope

It is intended with this study to explore ageing, a phenomenon that happens to old and/or regularly played instruments, described by various authors (Akahoshi et al., 2005; Bucur, 2016; Hunt & Balsan, 1996; Hutchinson, 1995; Inta et al., 2005; Obataya, 2017). Explanations range from small adjustments made to the instrument by musicians in time of use, natural ageing and change of properties of wood with time, long term static loading of the system and the effect of vibrations. The scope of this project is to study solely the effect that vibrations have on the dynamic response of the guitar system. In the context of this report, it is presented a small description of the mechanical system of the guitar, its dynamic response, and a critical analysis of previous studies. It is within this review of scientific data that the project scope will be refined to then define the methodology needed to fulfil the objectives of this project.

### 2.2. Brief history of the classical guitar

Since early history of human society stringed instruments have been used to produce sound. It is speculated by archaeologists that bows were the first crude form of stringed instruments (French & Bissinger, 2001). Similar instruments, such as the *berimbau*, have persisted to this day, coupling the bow with a crude sound chamber.

During the medieval ages, mainly in Europe and the Middle East, important breakthroughs in instrument design were made and applied to the strings and shape (such as a more complex resonance body) of said instruments. Basic lutes and gitterns were precursors to what we know today as the guitar, as seen in Figure 1. This evolution led to a refined design during the Renaissance and Baroque period (1600-1750), where the model for violins and guitars became more consistent and roughly similar to actual form (Chanan, 1994).

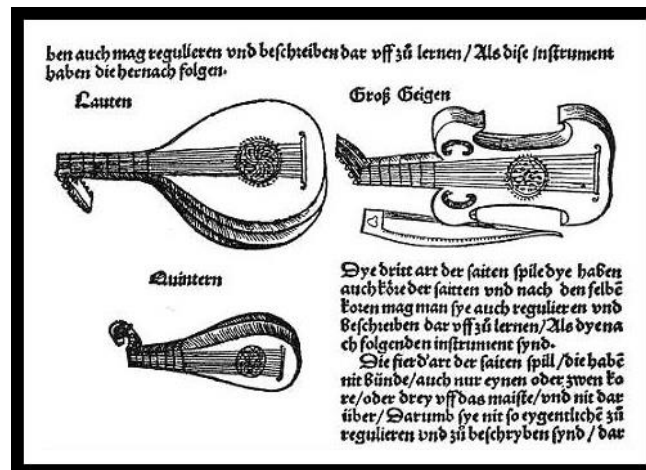


Figure 1 Early forms of string instruments (Virdung, 1511)

It was not until the 19<sup>th</sup> century that string instruments became more widely available through the means of mass production, becoming a standard part of chamber music and orchestras. In figure 2 we can observe one of the first modern shaped guitars.

Today the most common and widely available stringed instruments are part of the violin family (such as the viola, cello and bass) and the guitar family (French & Bissinger, 2001). These are the instrument families considered in this study as both share common mechanics and similar geometry which will be described in the subchapter 2.3.



Figure 2 Early Romantic guitar (ca.1830, Paris)

### 2.3. Mechanics of classical guitars

The basic sound producing mechanisms of stringed instruments are similar between them. Kinetic energy from vibrating strings propagates through the structural connections to the body which responds to this forced vibration. This dynamic is strongly

conditioned by the presence of an enclosed volume of air, usually with one or two ports to the outside part. Thus, the resulting sound radiated by the instrument is produced by the interaction between the structure and the air inside and outside of the instrument. For the violin and guitar family, this consists of a structure capable of holding a set of strings under a desired tension and an acoustic cavity with a flexible top and back to radiate sound.

Concerning classical guitars, they are manufactured in a wide range of sizes, designs and materials but share a set of common basic features. The body is usually made of wood with the possibility of adding a significant portion of composite material. The top plate is very thin and stiffened on the inside with wood braces. Different patterns, symmetrical or asymmetrical, as seen in figure 3, can be applied mounting the braces and are a matter of great discussion. Vibrational mode shapes at low frequencies will remain similar even with different bracings (Rossing, 2010).

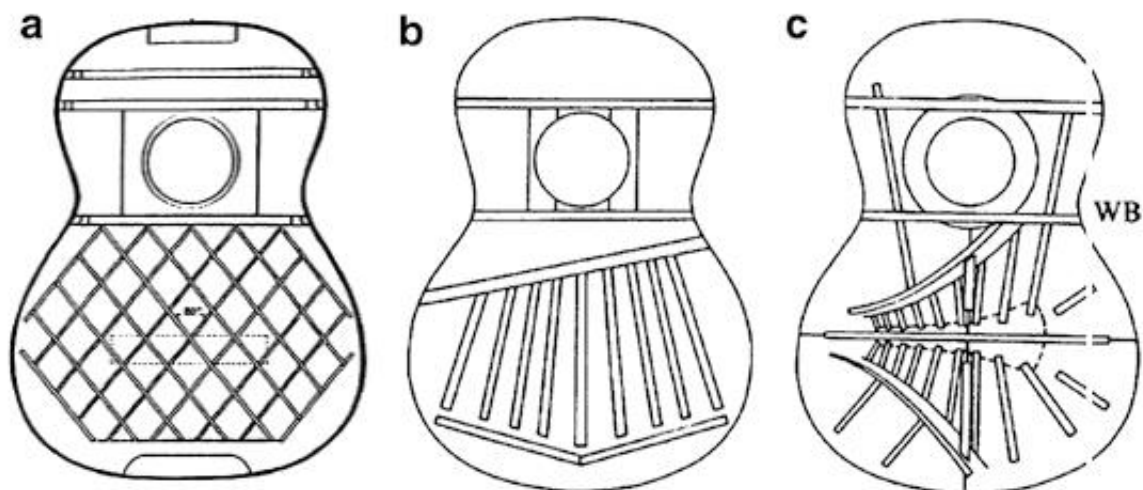


**Figure 3** Examples of symmetrical and asymmetrical top plate patterns: (a) Smallman (Australia); (b) Fleta (Spain); (c) Eban (USA) (Rossing, 2010)

The structure must be a careful balance between flexibility and stiffness. Flexible enough to deform in response to the string vibrations but stiff enough to resist the static load imposed by string tensions. This tension is variable with the use of different materials and diameters in the string set-up. Usually nylon strings will be used for classical guitars and higher pitched strings will have smaller diameters, this way the tension is on the same order of values for all six strings, around 35-45 Newtons per string (French & Hosler, 2001). This load is supported by both body and the neck.

The neck may be described as a cantilevered beam, even if the boundary condition is only approximately clamped. A reinforcement made of steel or graphite may be applied to increase stiffness, as seen in figure 4 (French & Hosler, 2001).

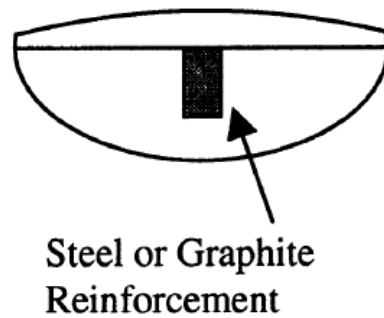


**Figure 4** Classical guitar neck cross-section (Rossing, 2010)

The sound hole constitutes a port for the enclosed air in the body, making it work as a Helmholtz resonator (Rossing, 2010). It is usually located in the centreline of the instrument between the neck and the bridge (other designs have been made but were never popular). Because of its location, the braces and top must transfer the string loads around it. In figure 5 a diagram of a classical guitar is presented naming all the main components.

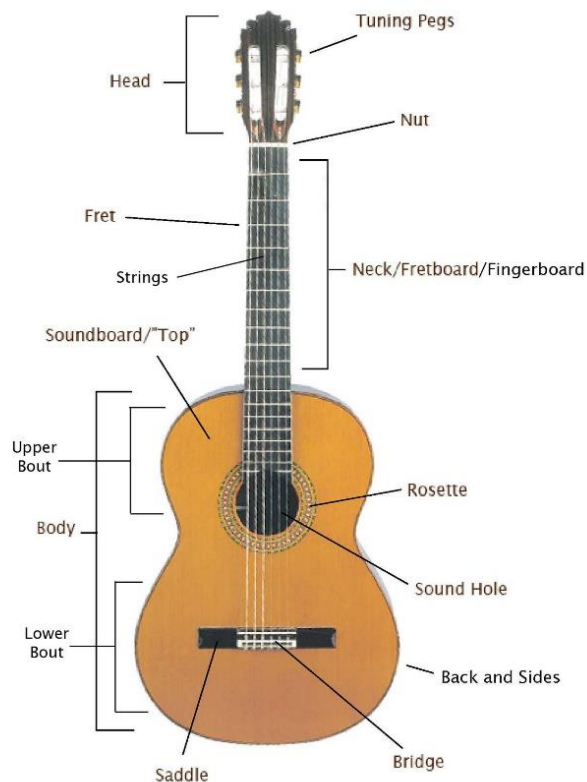


**Figure 5** Detailed anatomy of a classical guitar

## 2.4. Dynamic and modal response of classical guitars

Due to different body geometry and different bracing designs modal response will be different for different guitars. This is true except for the first modes which are generally similar (Rossing, 2010).

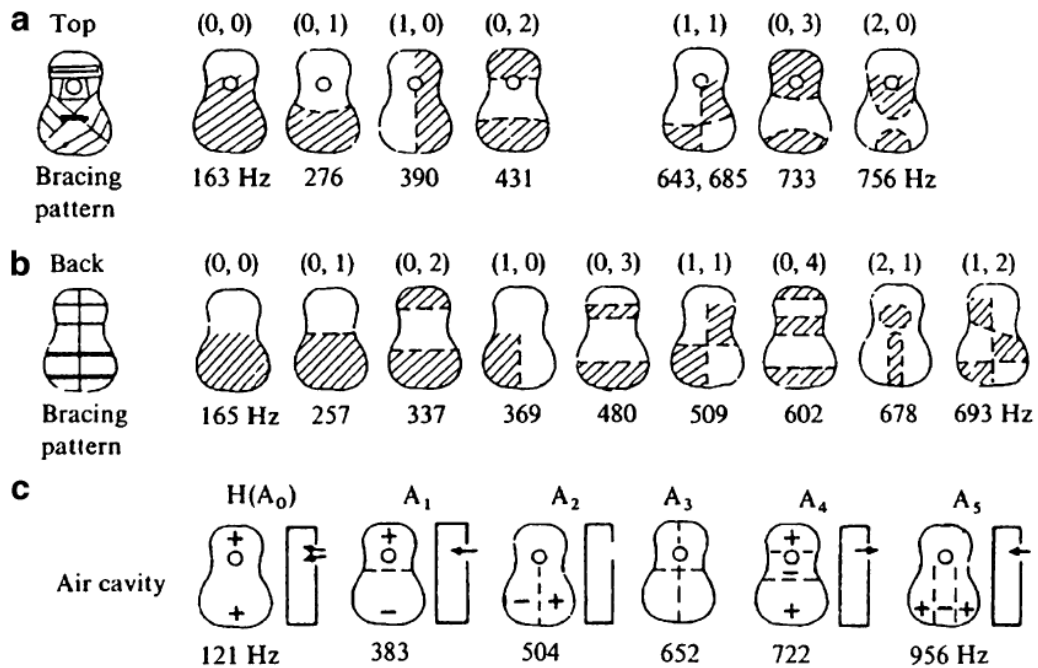


Figure 6 Top Plate, Back Plate and Air vibration modes (Rossing, 2010)

The individual modes for both the plates and air are presented in figure 6. The coupled system of the top plate, back plate and air will usually acquire one first mode known as the breathing mode ( $A_0$ ) which is characterised by having no nodal lines, in which the top and the back will vibrate in opposing phases, similar to a “breathing” movement. Other modes known as (0,0), as seen in figure 7, may be found for low frequencies (Rossing, 2010). They are characterized for being a coupling between the air modes and the modes from the plates.

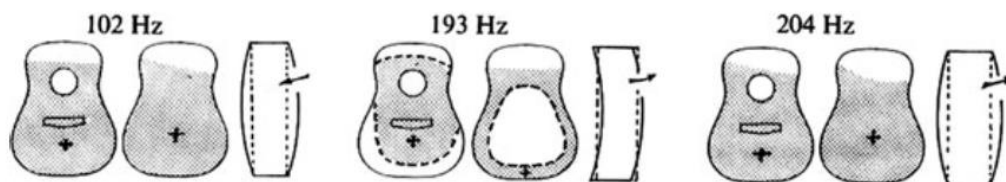
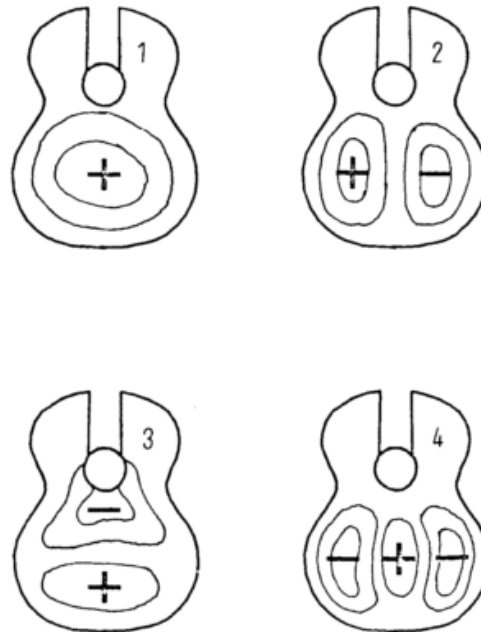


Figure 7 Breathing modes of a freely supported Martin D-28 guitar in the low frequency region (Fletcher & Rossing, 1998)

As the frequency goes higher, vibration modes will have less coupling between these elements, and most of the observed resonances are due mainly to vibration in the top

plate. The first three observed modes of vibration, as seen in figure 8, are similar in various sources (Christensen, 1984; Elejabarrieta, Ezcurra, & Santamaría, 2002; Rossing, 2010; Van Karsen, 1997).



**Figure 8** First vibrational modes found in most classical guitars (Christensen, 1984)

## 2.5. Concept of sound quality and instrument ageing

The quality of sound of a musical instrument is a hard to define and subjective area. Words like sound projection, note clarity, sonic balance, sustain and others have been used in describing the quality of sound (French & Hosler, 2001; Inta et al., 2005). Attempts to describe sound quality physically have been made (Howard & Angus, 2001; S. Šali & Kopač, 2000) making it directly associated with the vibrational modes and the efficiency of sound radiation of instruments. Mechanical and structural properties will influence instrument sound and it is often desirable to have a high stiffness to weight ratio and low damping coefficients (Inta et al., 2005).

Observing a frequency response function (FRF), being the FRF of an instrument the magnitude of the response to a stimulus at a given frequency, the concept of a good and bad guitar have been associated to the amplitude and damping of the peaks of resonance, being desirable a high amplitude of resonance and a low damping coefficient, as seen in figure 9 (S. Šali & Kopač, 2000).

Along with various factors and external variables such as room temperature and humidity, or the history of usage and maintenance of the instrument, sound quality may

increase or decreased with time. One of those variables is the ageing of instruments which is a wide-spread belief that instrument sound improves with age and regular playing (Akahoshi et al., 2005; Hunt & Balsan, 1996; Hutchins, 1998; Inta et al., 2005; Obataya, 2017).

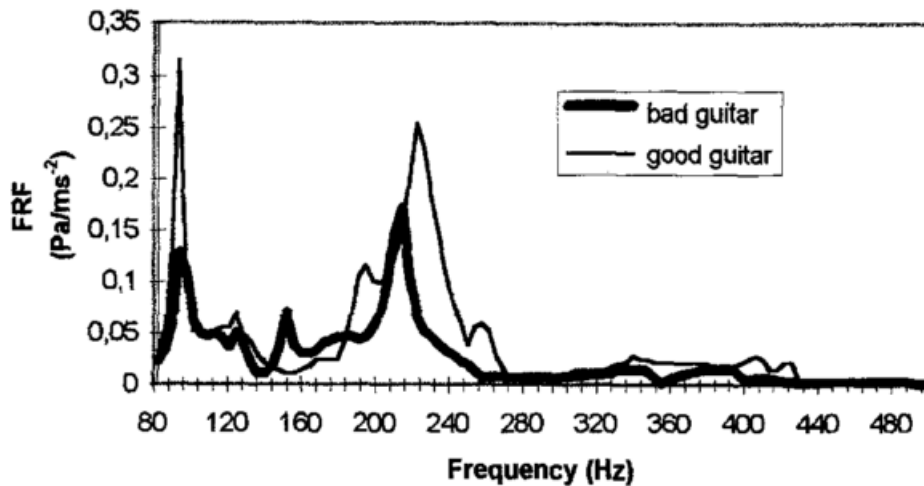


Figure 9 Frequency response function for a bad and good guitar (S. Šali & Kopač, 2000)

Several hypotheses have been suggested to explain instrument ageing and to why it improves sound. Some of which are not directly linked with changes in intrinsic properties but with small adjustments made by the musician to a regularly played instrument, such as changes of the bridge, the type of strings etc. making the instrument constantly evolve towards a better sound and playability (Inta et al., 2005).

Other explanations focus on the change of wood properties and structure with age, referring to the ageing that occurs in polymers, considering wood as a natural polymer. Physical ageing of polymers is defined as “the observed change in a property of the polymer as a function of storage time, at constant temperature and zero stress, and under no influence from any other external conditions” (Hutchinson, 1995). These changes occur in the macrostructure and microstructure, influencing viscoelastic properties. In the context of musical instruments, the “natural ageing of wood” makes a much more complex problem if we take into account all the different factors and interactions with its environment, such as the variations of air humidity and chemical interactions of the components of wood with air, ultraviolet energy, pollutants, musicians’ hands, microorganisms, etc.

For an ageing instrument that is regularly played, one must consider the main mechanical stresses induced in musical instruments which are long term static loading and vibrations. Long term static loading induces creep in the wood which presents three types

as noted by Hunt (1999): viscoelastic creep which is time dependent, mechano-sorptive which relates to changes in internal moisture, and pseudo-creep related to differential swelling and shrinkage of wood.

Concerning vibrations, a previous study has shown measurable mechanical differences both in regularly played instruments and vibrated instruments, being that the vibrated instrument has shown less overall change (Hutchins, 1998). Another study shown that for beams of spruce, in a controlled environment, continuous forced vibrations caused the increase of stiffness and the decrease of the damping coefficient by about 5% on average (Hunt & Balsan, 1996). These authors have suggested that the explanation for this may lie in a redistribution of moisture and water molecules, induced by vibrations, from high energy and high strain sites to lower energy sites.

Other authors have mentioned characteristics of newly made or repaired instruments which are harmful to sound quality and may be improved through means of vibration (Bucur, 2016). The glue used in a freshly made instrument forms a macromolecular, gel-like compound material with unneglectable inelastic characteristics, which affects the coupling between the different body parts, such as the connection between the ribs and the front and back plate, an area which should be flexible. In a similar way, the varnish used in finishing the instrument introduces a viscous and inelastic layer over the wood. This makes for a significant amount of inelastic material by volume, resulting in local tensions that lead to losses in the applied vibration energy. This means that vibration modes may be partially blocked, and some may suffer from an acoustical “short-circuit”. Analog to heat treatments which removes deformation stresses from structures and welded connections of materials, one can apply a similar principal to instruments (Bucur, 2016). Vibration promotes the redistribution of particles to lower energy sites, such as the adsorbed water molecules. A relaxation is also suggested, as a periodically varying stress applied to a polymer will be converted from a mechanically applied work into heat energy due to the viscous motion resistance. Theoretically, if the stress cycle amplitude of vibration is great enough, the viscosity will be altered in a direction that reduces damping, thus improving instrument sound.

To summarize instrument ageing, improvement of sound with instrument age may come from small adjustments made by the musician, natural modification of wood that comes with age and exposure to the environment, playing and vibration related mechanical changes to the properties of wood, and vibration related improvements to the whole guitar body system with the relaxation of connections between body components. Sound quality

will be improved by the increase of stiffness, reduction of damping, full activation of vibration modes and increase in sound radiation.

## 2.6. Previous related studies

### A measurable effect of long-term playing on violin family instruments (Hutchins, 1998)

The body of violins became more flexible as result of long-term vigorous playing by increased amplitude of the cavity resonances in response to constant input signal.

A small-sized microphone and loudspeaker have been introduced in the instrument sound holes. Then, from the loudspeaker, a sine wave at constant amplitude sweeps the frequency range from 0.1 to 10 kHz, to which the microphone registers the resulting air pressures.

For a cello played from 1990 to 1994 it is possible, in figure 10, to observe that the A1 cavity mode has increased 7 dB, the peak at 831 Hz has increased 10 dB, and in general peaks above that frequency have all increased. This means the instrument is effectively producing a louder sound in general.

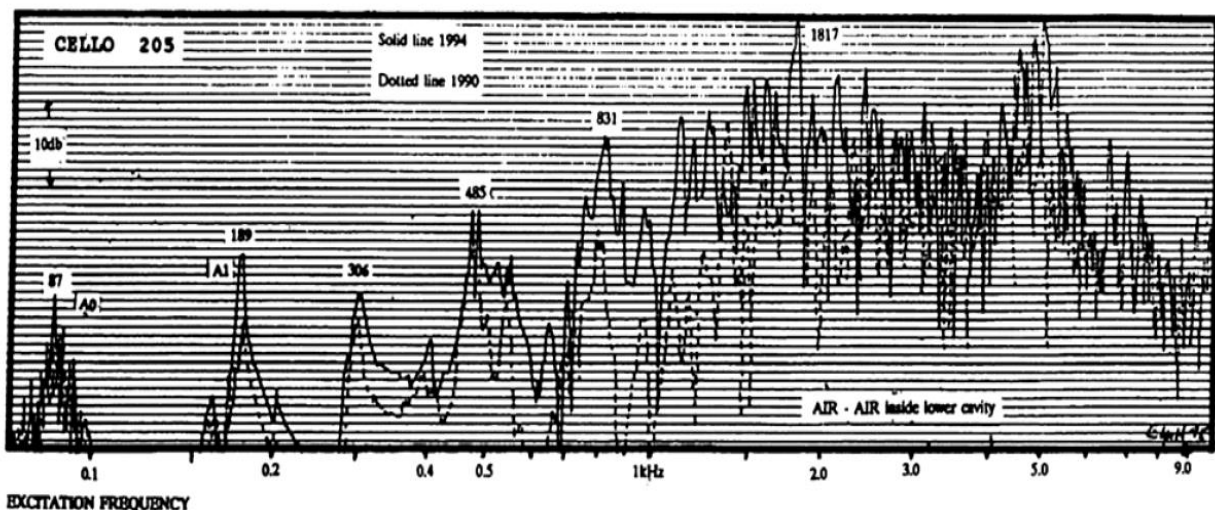


Figure 10 Sound pressure for excitation frequency of a cello after 4 years of playing (Hutchins, 1998)

The same has been observed for a viola played for three years. Another violin was played infrequently between 1987 and 1995 but was subjected twice to a 1500-hour vibration test coming from a classical radio station. Measurable differences, as seen in figure

11, were noticed but not as strong. The author suggests that further experimentation should be done in this matter.

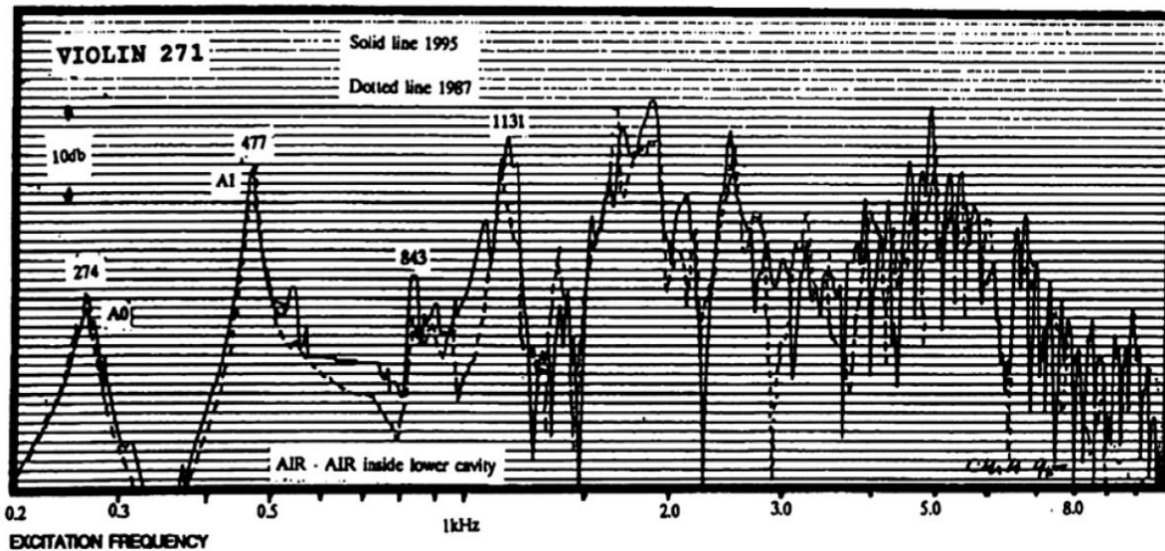
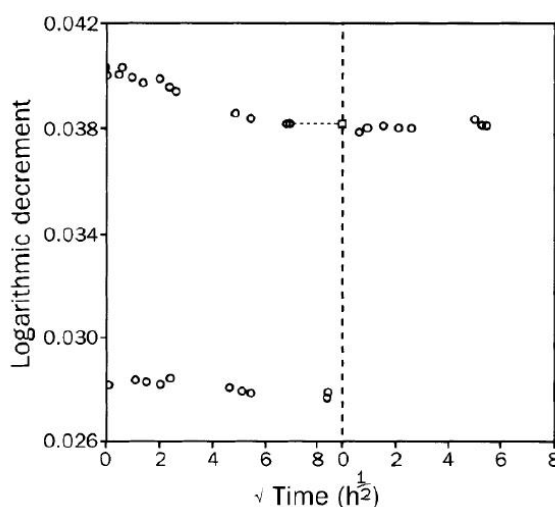


Figure 11 Sound pressure for excitation frequency of a violin subjected to vibration tests (Hutchins, 1998)

### Why old fiddles sound sweeter (Hunt & Balsan, 1996)

Beams of spruce were subjected to a continuous vibration at the natural frequency of 10 Hz. It was observed, as seen in figure 12, that the damping coefficient drifted downwards by about 5% on average, sometimes after a small increase. When the forced vibrations ceased there was little or no change. The forced vibrations also caused an increase in the natural frequency of about 0.3%. The effect was more noticeable at high humidity. The authors suggest that the observed effect may lie within mechanisms of moisture bonding, with water particles contained in wood being redistributed from high energy, high strain locations to lower energy sites.



Damping coefficient expressed as logarithmic decrement plotted against the square root of time during forced vibrations at the natural frequency of a spruce cantilever beam of dimensions 85 mm (axial) by 12 mm (radial) by 0.5 mm (tangential), at 90% RH (upper) and 44% RH (lower). The vibrations were switched off after 48 h. Left, with vibrations; right, vibrations stopped. Measurements were made following moisture equilibration (to an estimated tolerance of 0.3%). The time at equilibrium humidity was at least 16 times the measured sorption time constant. At 90% RH, the experiment was continued by switching off the vibrations after 48 h. The coefficient of variation of the measurement technique was 0.35% for the damping coefficient and 0.0065% for the frequency. The humidity of the environmental chamber was maintained within  $\pm 1\%$  RH and  $\pm 0.1$  °C. The measurements made during continuous forced vibrations at constant humidity were made six times, on matched samples.

Figure 12 Variation of the damping coefficient with forced vibrations (Hunt & Balsan, 1996)

### Effects of continuous vibration on the dynamic viscoelastic properties of wood (Akahoshi et al., 2005)

A previous study (Sobue & Okayasu, 1992) measured the evolution of the dynamic Young's Modulus ( $E'$ ) and loss tangent ( $\tan\delta$ ) for different species of wood during continuous vibration. While  $E'$  remained constant, significant reduction of  $\tan\delta$  was observed. The loss tangent is a common measure of viscoelasticity in the dynamic range used in the study of wood properties (Havimo, 2009). The lower the loss tangent, the lower is the dissipation of mechanical energy, which translates as less damping.

It was speculated by Sobue and Okayasu (1992) that certain internal stress was induced by the drying of green wood, and that the application of vibration caused a relaxation of such "drying stress". In figure 13 the authors present the viscoelastic model that explains the drying stress and relaxation, being (a) the viscoelastic part consisting of amorphous polymers; (b) adsorbed water in the amorphous region; (c) crystalline cellulose.

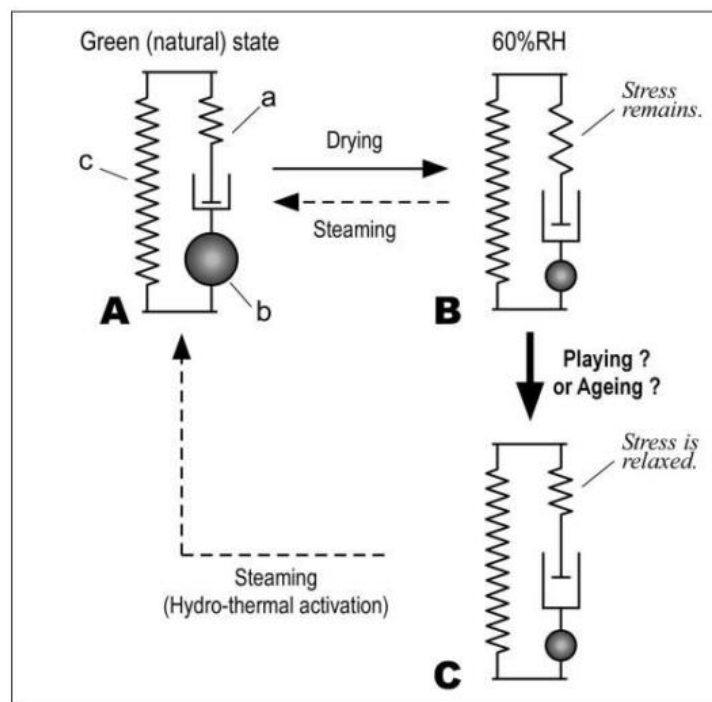


Figure 13 Viscoelastic model (Akahoshi et al., 2005)

To test this mechanism that explains the effect of vibrations on wood, the authors suggest that a piece of green wood or hydro-thermally treated wood, where no drying stress exists, will suffer no consequences from continuous vibration.

Two pieces of Sitka Spruce wood were tested, one was a steamed wood sample and the other was kept at 25°C and 60% relative humidity.

The results, as observed in figure 14, show an increase in  $E'$  and decrease of  $\tan\delta$  during vibration for the dry specimen, to values that remained unchanged after the vibration treatment. Note that the  $y$ -axis is expressed as percentage change in property and both samples begin at 0%. For the steamed sample, continuous vibration affected little  $E'$ , which implies that the playing effect is related to the relaxation of drying stress. The authors suggest the decrease in  $\tan\delta$  might be explained by an insufficient short steaming treatment, or the addition of thermal stress by the cooling after the steaming treatment, which can also be relaxed by continuous vibration. We must note that the authors gave no information about the type of continuous vibration applied. The authors suggest that further detailed experiments are necessary to prove the contribution of drying stress.

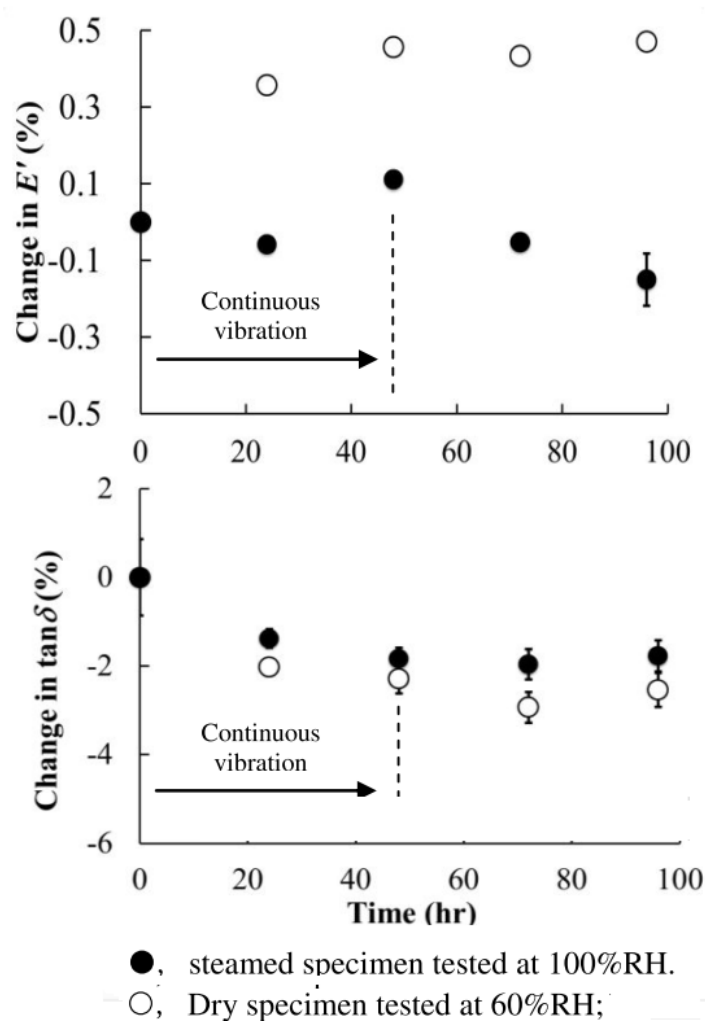


Figure 14 Change of  $E'$  and  $\tan\delta$  in time (Akahoshi et al., 2005)

### **Effect of Vibration Treatment on Guitar Tone: A Comparative Study (Clemens et al., 2014)**

This study compares three pairs of guitars, each pair being the most similar possible – same maker, same model, made on the same year. From each pair, one is kept untouched, in the same room as the other, for control, and the other is subjected to a vibration treatment that comes from a commercially sold device for tone improvement. This device imposes a 60 Hz vibration to the strings of the guitar, which transmits the vibration to the rest of the guitar system. The guitars subjected to the treatment had the devices transmitting the mentioned vibration for 348 hours. Several different tests were used for analysing guitar responses. One of which made use of a calibrated impact hammer to impart an impulse to the guitar's top plate. The response was measured using a calibrated accelerometer, mounted with wax on the guitar center line. Both the time response of the input hammer and top plate accelerometer were recorded. The guitars were held in a cradle making contact only with the sides and middle of the neck, allowing for unhindered motion of the top plate and back plate. To avoid the ringing of the strings, foam dampers were used to damp the strings.

Each modal analysis was performed on each guitar before and after the vibration treatment. The post-treatment test sessions were performed 16 hours after stopping the vibration treatment. New strings were applied to each guitar on the night before the two test sessions.

The analysis of the data obtained was made through an FRF. This function is frequently used for analysing and comparing instruments, as seen in other studies (Inta et al., 2005). Fourier analysis is used to obtain the FRF from the time domain signals, in which:

$$s(t) = h(t) * r(t) \quad (2.1)$$

$s(t)$  is the output,  $h(t)$  the force and  $r(t)$  the impulsive response.

Taking the Fourier transform:

$$F[s(t)] = F[h(t)] \cdot F[r(t)] \quad (2.2)$$

so, the frequency response function of the guitar is as follows:

$$R(f) = \mathcal{F}[r(t)] = \frac{\mathcal{F}[s(t)]}{\mathcal{F}[h(t)]} \quad (2.3)$$

To compare the different FRFs, Pearson's  $r$  correlation coefficient was used, given by the following standard expression:

$$r = \frac{\sum_n (R_1(n) - (R_1)) (R_2(n) - (R_2))}{\sqrt{\sum_n (R_1(n) - (R_1))^2} \sqrt{\sum_n (R_2(n) - (R_2))^2}} \quad (2.4)$$

where  $R_i(n)$  is the  $n$  frequency data point for the  $i$  frequency response function and refers to sample average of the quantity. Pearson's  $r$  measures the correlation, or linear dependence, between two variables, in this case between the FRFs of different guitars, quantifying the changes in guitars before and after treatment, in which  $0 < r < 1$ , being 0 no correlation and 1 perfect correlation. It is then expected that guitars subjected to treatment to have a lesser  $r$  value than their non-treated counterparts. This correlation varies with the maximum frequency used, becoming unreliable above 5 kHz, making the used FRF to be in the 0 Hz – 5 kHz interval.

Analysing the FRF data, shown in figure 15, where for each pair guitar A is the untreated guitar and B the treated guitar, the obtained Pearson's correlation for the 0-1000 Hz interval is shown in table 1. The pure statistical uncertainty was in the range of 0.01-0.02 and larger for smaller correlation coefficients, with the authors concluding that changes of a percent or two are probably not significant. As one can read in the paper about Table 1: "The bold, italicized numbers are comparisons between the same guitar before and after the treatment. The plain numbers are comparisons between different guitars before the treatment, and the italicized, non-bolded numbers are comparisons between different guitars after the treatment".

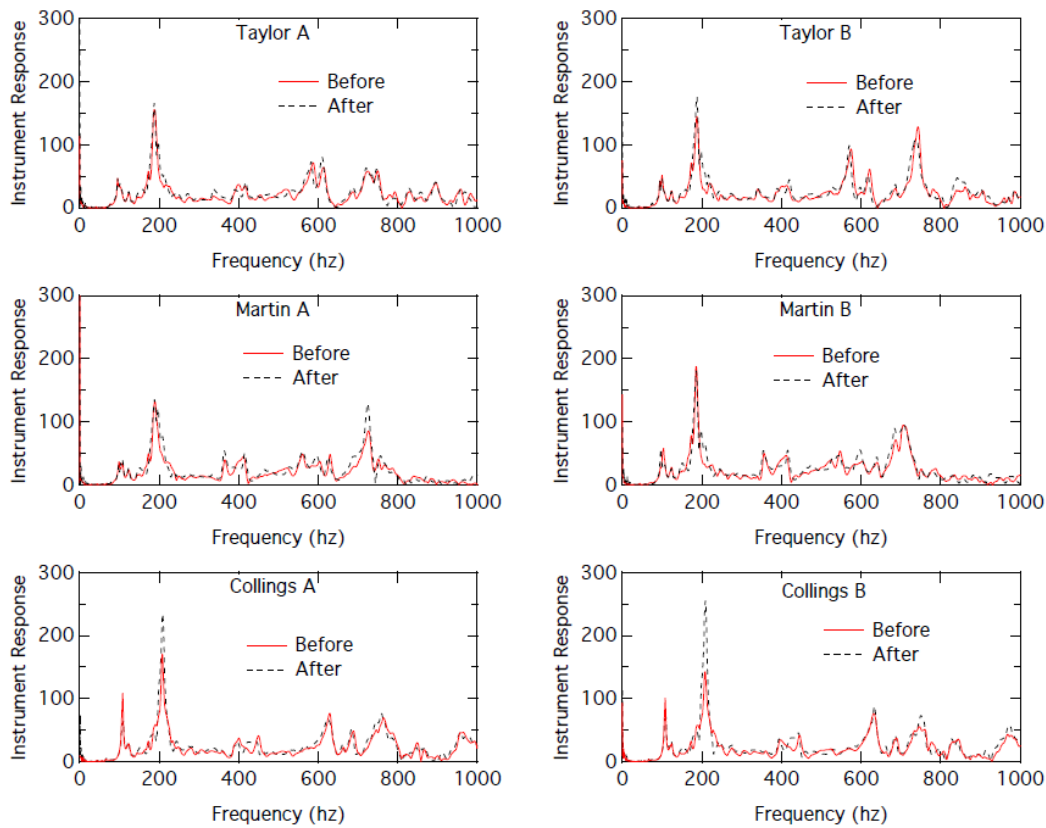


**Figure 15** Frequency response functions obtained for the guitar pairs (Clemens et al., 2014)

| vs       |   | Taylor      |             | Martin      |             | Collings    |             |
|----------|---|-------------|-------------|-------------|-------------|-------------|-------------|
|          |   | A           | B           | A           | B           | A           | B           |
| Taylor   | A | <b>0.92</b> | 0.84        | 0.75        | 0.69        | 0.40        | 0.40        |
|          | B | 0.81        | <b>0.89</b> | 0.72        | 0.60        | 0.39        | 0.35        |
| Martin   | A | 0.79        | 0.70        | <b>0.93</b> | 0.80        | 0.45        | 0.43        |
|          | B | 0.69        | 0.59        | 0.81        | <b>0.93</b> | 0.29        | 0.29        |
| Collings | A | 0.41        | 0.39        | 0.47        | 0.27        | <b>0.92</b> | 0.95        |
|          | B | 0.45        | 0.45        | 0.50        | 0.30        | 0.92        | <b>0.90</b> |

**Table 1** Pearson’s Correlations (Clemens et al., 2014)

The conclusion is that there is no significant difference between the changes in non-treated guitars as well as for the treated guitars. For all six guitars the Pearson’s correlation coefficient is about  $0.91 \pm 0.02$  before and after the treatment.

Before this analysis, the authors experimentally determined that the magnitude of the acceleration during the vibration treatment using the commercially available device is about 100 times smaller than that of one gentle guitar strum with a guitar pick, as observed in figure 16. Also, the frequency of vibration treatment, 60Hz, is significantly different from the frequencies produced by a strum. This means that the vibrations imposed by the device are much softer than those expected from regular guitar playing and do not represent realistic guitar playing.

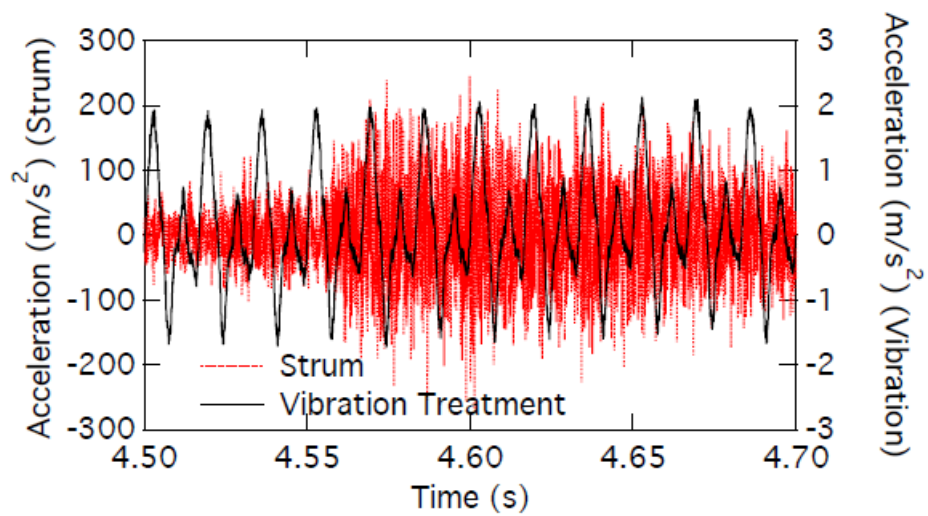


**Figure 16** Output of the guitar-top mounted accelerometer as function of time during a gentle strum from a strumming device and during vibration treatment (Clemens et al., 2014)

With this observation the authors conclude nothing about the outcome of a more vigorous vibration treatment, suggesting further experimentation in this area.

### **3. EXPERIMENTAL MODAL ANALYSIS**

Modal analysis is regarded as a way of describing a system through its natural vibrational characteristics, known as modal parameters, which are the natural frequencies, their damping and mode shapes. These values give an important insight on how structures behave in response to excitations. This chapter will provide an overview of the application of experimental modal analysis in general/industrial cases, how it can be applied to music acoustics and how it will be applied for this study.

#### **3.1. Industrial applications**

Noise and vibrations are a common occurrence in industrial applications. Dynamic forces excite structures which respond in the form of noise and vibrations. For humans, effects may range from simple annoyance, to more serious health and safety hazards. For machines these can result in reduced life and performance, faulty operation and irreversible damage. Most of these problems are due to resonance, which occurs when dynamic forces excite the structure's natural frequencies. This is especially problematic when modes of vibration are within the frequency range of operational dynamic forces. To predict structural response and improve designs, modal analysis takes place.

Modal analysis, which can be done in an analytical and experimental way, determines the modal parameters which can be used for analysis or to formulate mathematical dynamic models for prediction of behaviour.

Analytical mathematical models are obtained based on the structural matrices: mass, stiffness and damping and are usually calculated with Finite Element Method.

Mathematical models with experimental data are constructed based on the measured system response, which can be analysed in both the time domain, and in the frequency domain, e.g. FRF. Then modal analysis identification methods are used for the identification of the modal parameters (Avitabile, 2001; Kerschen & Golinval, 2000).

The modal parameters, found by both methods, can be directly compared and used to adjust and refine the analytical model. In such a way, the refined analytical model can then be used to predict the response of the system to different forces. An example of this application in the construction industry is illustrated in figure 17, in which the analytical and experimental models are obtained for a building. The refined analytical model is used to predict the structural response to design forces, evaluate and improve the safety and comfort of the occupants of the building.

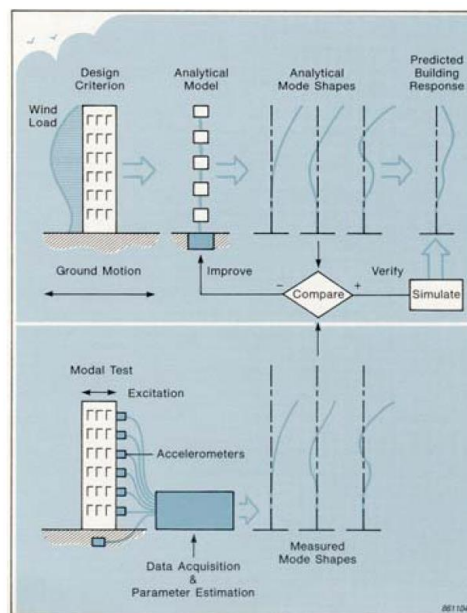
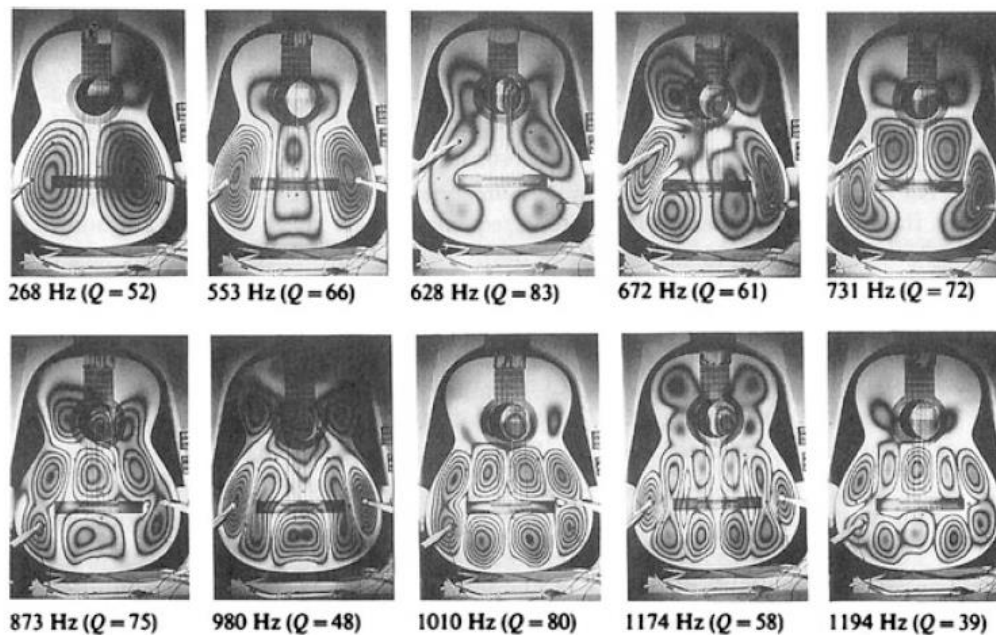


Figure 17 Analytical and experimental modal analysis of a building (Døssing, 1988a)

### 3.2. Applications in Music Acoustics

Music acoustics, specifically the branch that dedicates to the physics of musical instruments, makes use of modal parameters to analyse the instrument vibrational behaviour. Due to the specific characteristics of instruments, being complex and fragile systems, different approaches have been developed.

Chladni powder patterns, holography and laser interferometry have proven to be useful in observing the resonance phenomena on the top plate of guitars, violins and other instruments (Firth, 1977; Hutchins, Stetson, & Taylor, 1971; E. Jansson, 1969; E. V. Jansson, Molin, & Sundin, 1970). A study of the complete resonance box has been made, also with holography, under free boundary conditions (Richardson & Roberts, 1985). In figure 18 we can see the mode shapes and corresponding frequencies are well identified for a classical guitar.



**Figure 18** Holographic interferograms of a classical guitar (Richardson & Roberts, 1985)

Frequency response functions have been used to analyse instrument response and compare instruments, by means of observing the resonance peaks, which correspond to the natural frequencies of the instrument (Hess, 2013; Inta et al., 2005; Samo Šali, 2002; Samo Šali & Kopač, 2000). These can provide an insight on the quality of the instrument and investigate how modifications to the system and parts of the instrument will affect responsiveness, as FRF is a quantitative measure of an output in response to the input inserted into the system.

Further studies have developed mathematical models, using finite element methods and experimental modal analysis, which are complementary as their results can be compared and used to confirm and improve the theoretical mathematical model (Bretos, Santamaría, & Moral, 1999; Elejabarrieta et al., 2002; Knott, 1989; Tapia, 2002). While modal analysis technique allows to study the behaviour of the instrument as a whole, numerical calculations from finite-element make possible to study in detail the components of the system.

### 3.3. Modal identification technique

The subject of our study is a modern classical guitar, property of Professor Paulo Vaz de Carvalho, which has not been regularly played since its construction 20 years ago, but nonetheless carefully stored and maintained. This makes a good sample for the study on the influence of vibration on guitar tone, since it's an aged guitar, suffering no major repairs or reconstructions, and has suffered little vibration during its lifetime. Experimental modal analysis will be applied to follow the evolution of the vibrational behaviour of the guitar as a whole, proving or disproving non-neglectable effects of vibration. There are several ways to do this: one must first acquire a system response, and then apply a convenient modal identification method to obtain modal parameters.

Modal analysis identification techniques can be classified (Kerschen & Golinval, 2000) according to:

1. The domain of the measured system response, which can be in the time or frequency domain.
2. Whether it is a single-degree-of-freedom (SDOF) or a multi-degree-of-freedom (MDOF) method, depending on the number of modes considered in the analysis.
3. Single-input-single-output (SISO), single-input-multi-output (SIMO), multiple-input-multi-output (MIMO) methods depending on the capacity of the method to deal with several response locations.

In the time domain generally, it is not possible to separate contributions from different modes and it is only possible to do a MDOF analysis.

In the frequency domain the accuracy of results can be improved by adding residual members, but some problems such as leakage and closeness of natural frequencies justify the use of the time domain instead of the frequency domain (Kerschen & Golinval, 2000).

Several identification methods have been proposed in literature, some of the most common being, among other methods: the Least-Squares Complex Exponential method (Brown, Allemang, Zimmerman, & Mergeay, 1979), the Ibrahim Time Domain method (Ibrahim & Mikulcik, 1973) and Stochastic Subspace Identification method (Van Overschee & De Moor, 1996) in the time domain; the Least-Squares Frequency Domain method in the frequency domain which, must be used together with the Least-Squares

Complex Exponential method (Brown et al., 1979) to obtain an estimation of the mode shapes.

For this study the selected method is the Eigensystem Realization Algorithm (ERA) (Juang & Pappa, 1985), for it is a modern, NASA developed, efficient method capable of working with structures that present complex dynamic behaviour.

### 3.3.1. Eigensystem Realization Algorithm's formulation

The ERA method has two main steps: first, the model reduction of the dynamical systems and then, the identification of the modal parameters (Juang & Pappa, 1985).

A time invariant, linear, of finite dimension dynamic system, with  $N$  degrees of freedom may be represented by the system of second-order differential equations:

$$[M]\{\ddot{y}(t)\} + [C]\{\dot{y}(t)\} + [K]\{y(t)\} = \{f(t)\} \quad (3.1)$$

where  $[M]$ ,  $[C]$  and  $[K]$  are the mass, damping and stiffness matrices,  $\{\ddot{y}(t)\}$ ,  $\{\dot{y}(t)\}$ ,  $\{y(t)\}$ , are the acceleration, velocity and displacement vectors, and  $\{f(t)\}$  is the load force vector. In our study we are using ERA SISO method for an impulse response.

Assuming the responses sampled at time  $t_k = k\Delta t$  with  $k = 1, \dots, K$  and using a state-space representation for the dynamics, equation (3.1) can be rewritten as:

$$\{x_{k+1}\} = [A_d]\{x_k\} + [B_d]\{u_k\} \quad (3.2)$$

$$\{y_k\} = [C_d]\{x_k\} + [D_d]\{u_k\} \quad (3.3)$$

for  $k = 0, 1, 2, \dots$

Considering an impulse excitation- expressed as a Dirac delta function – for the inputs as

$$\{u_k\} = \begin{cases} I, & \text{for } k = 0 \\ 0, & \text{for } k > 0 \end{cases} \quad (3.4)$$

and assuming  $\{x_0\} = 0$ , one can write the impulse response  $\{y_k\}$  as:

$$\{y_k\} = \begin{cases} [D_d], & \text{for } k = 0 \\ [C_d][A_d]^{k-1}[B_d], & \text{for } k > 0 \end{cases} \quad (3.5)$$

where  $\{y_k\}$  are usually called the Markov parameters in the literature.

What the ERA tells us is that our modal parameters are contained within the matrix  $[A_d]$ . The first step to obtain the matrix  $[A_d]$  is to construct two Hankel matrices from the impulse response:

$$[H(0)] = \begin{bmatrix} [y_1] & [y_2] & \cdots & [y_k] \\ [y_2] & [y_3] & \cdots & [y_{k+1}] \\ \vdots & \vdots & \ddots & \vdots \\ [y_k] & [y_{k+1}] & \cdots & [h_{k+k}] \end{bmatrix} \quad (3.6)$$

$$[H(1)] = \begin{bmatrix} [y_2] & [y_3] & \cdots & [y_k] \\ [y_3] & [y_4] & \cdots & [y_{k+1}] \\ \vdots & \vdots & \ddots & \vdots \\ [y_k] & [y_{k+1}] & \cdots & [h_{k+k}] \end{bmatrix} \quad (3.7)$$

where  $y_k$  are the samples of the impulse response.

We can limit the size of our Hankel matrices to the interval of discrete time that we consider relevant for the identification, as not all of the capture time of our recorded signals has relevant information. Reducing the matrices will diminish the size and computation time.

The next step is to reduce the model order. To that end, we perform a Singular Value Decomposition of the matrix  $[H(0)]$ .

$$[H(0)] = [U][\Sigma][V]^T = [U_n \ U_p] \begin{bmatrix} [\Sigma_n] & 0 \\ 0 & [0] \end{bmatrix} \begin{bmatrix} [V_n^T] \\ [V_p^T] \end{bmatrix} \quad (3.8)$$

where  $[\Sigma_n]$  is the matrix of the singular values. This is our reduced order model since for our analysis the SVD is partitioned in accordance to the selected number of  $n$  largest singular values. An appropriate selection of  $n$  will provide us with enough information to obtain the  $[A_d]$  matrix.

Defining the matrices  $H_1$  and  $H_2$  as:

$$H_1 = U_n \Sigma_n^{-\frac{1}{2}} \quad (3.9)$$

$$H_2 = \Sigma_n^{-\frac{1}{2}} V_n^T \quad (3.10)$$

and noting the expressions for the left inverse  $H_1^+$  and right inverse  $H_2^+$  are:

$$H_1^+ = \Sigma_n^{-\frac{1}{2}} U_n^T \quad (3.11)$$

$$H_2^+ = V_n \Sigma_n^{-\frac{1}{2}} \quad (3.12)$$

the matrix of interest for the identification of the modal parameters is given by the expression:

$$[A_d] = H_1^+ H(1) H_2^+ \quad (3.13)$$

The modal parameters are then extracted from the eigenvalues of the matrix  $[A_d]$  according to the expressions:

$$w_n = \left| \ln \left( \frac{\lambda_n}{\Delta t} \right) \right| \quad (3.14)$$

$$\zeta_n = -\cos(\text{angle}(\ln(\lambda_n))) \quad (3.15)$$

Where  $w_n$  are the modal frequencies,  $\zeta_n$  the modal damping and  $\Delta t$  is the discrete time-step.

Next, for the identification of the mode shapes, we construct the following mathematical model for the impulse response:

$$h(t) = \sum_{n=1}^N A_n e^{\lambda_n t} + \overline{A_n} e^{\overline{\lambda_n} t} \quad (3.16)$$

in which  $A_n$  is the amplitude of the mode and:

$$\lambda_n = -w_n \zeta_n + j w_n \sqrt{1 - \zeta_n^2} \quad (3.17)$$

$$\bar{\lambda}_n = -w_n \zeta_n - j w_n \sqrt{1 - \zeta_n^2} \quad (3.18)$$

where now, we can introduce the values of  $w_n$  and  $\zeta_n$  previously identified.

Finally, the modal amplitudes  $A_n$  can be estimated by solving the following equation:

$$[h(t)] = [h_{mod}][A_n] \quad (3.19)$$

where

$$[h_{mod}] = \begin{bmatrix} [e^{\lambda_n t}] & [e^{\lambda_n t}] & \dots & [e^{\lambda_n t}] \\ [e^{\lambda_n t}] & [e^{\lambda_n t}] & \dots & [e^{\lambda_n t}] \\ \vdots & \vdots & \ddots & \vdots \\ [e^{\lambda_n t}] & [e^{\lambda_n t}] & \dots & [e^{\lambda_n t}] \end{bmatrix} \quad (3.20)$$

and for which the solution can be obtained by the pseudo-inverse of  $[h(t)]$  as

$$[A_n] = [h(t)]^{-1} [h_{mod}] \quad (3.21)$$

In order to observe the accuracy of the ERA identification, stability diagrams (Brown et al., 1979) have been used. Estimates of the natural frequency and damping are performed as a function of increasing the model order. As model order increases more modal frequencies are estimated, but the identification of the correct modal frequencies tend to stabilize. On the contrary nonphysical computation modes do not stabilize and can be eliminated out of the modal parameter data set. An example of a stability diagram can be observed on figure 19.

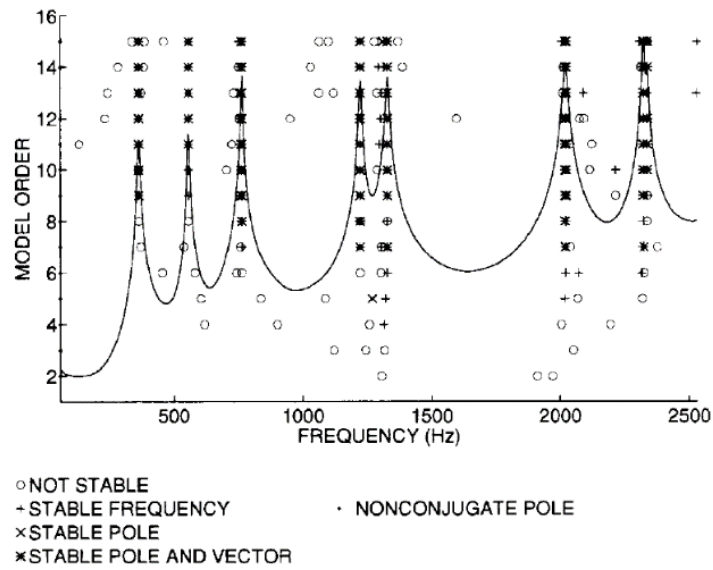


Figure 19 Stability diagram (Brown et al., 1979)

### 3.3.2. Experimental Set-up

A similar set-up to Clemens et al. (2014) has been used in order to obtain the necessary transfer functions for modal identification. An input and output signals are to be recorded with the guitar system in a boundary free set-up so there is minimum constraint to guitar vibration. To obtain this, the guitar has been freely suspended from the ceiling using elastic rope as seen in figure 20.



Figure 20 Free-boundary guitar set-up

A complete diagram of the experimental set-up for modal identification can be seen in figure 21.

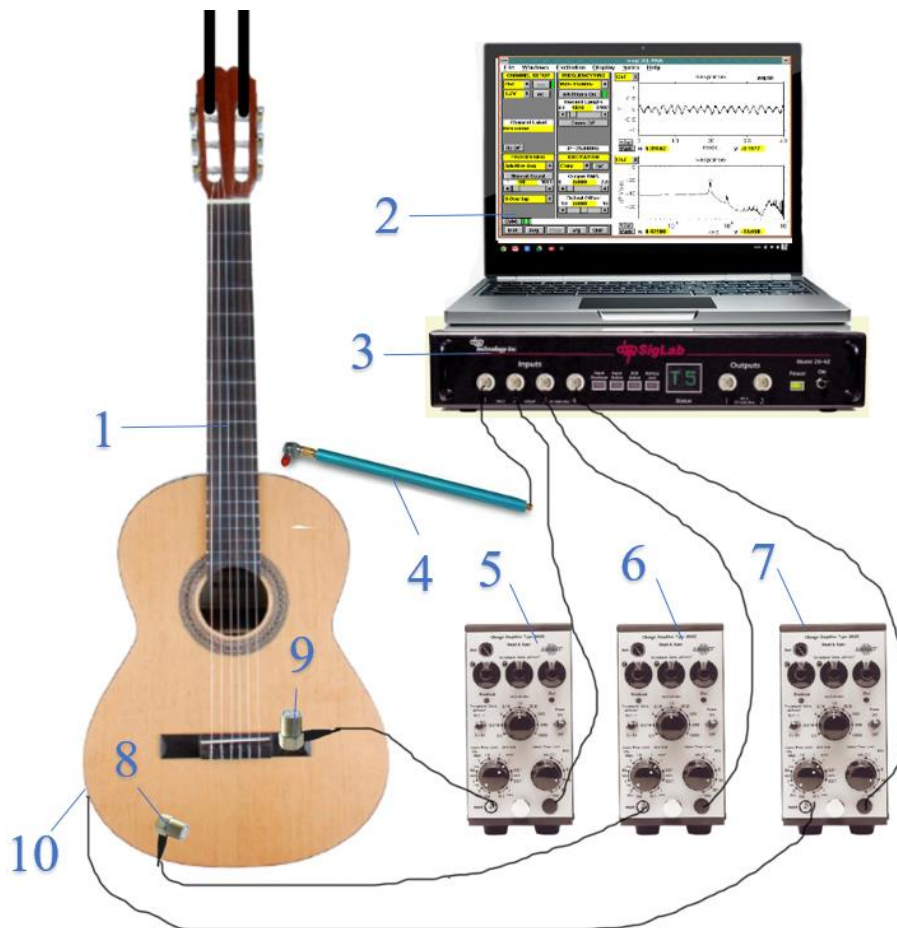


**Figure 21** Illustrative diagram of the experimental set-up for modal identification

The material presented on the diagram is as follows: (1) Guitar; (2) Laptop with acquisition software; (3) Siglab digital acquisition card (Spectral Dynamics model 20-42); (4) Piezotronics Miniature Instrumented impulse hammer; (5)-(7) *Bruel & Kjaer* type 2635 Pre-amplifiers; (8)-(10) Miniature piezoelectric *Bruel & Kjaer* 4375 charge accelerometers.

The methodology is simple but meticulous to be precise. Our excitation consists of an impact excitation done with the help of the impulse hammer. This produces a waveform which is a transient energy transfer event. The useful frequency range is from 0 Hz to an upper limit of frequency  $F$  at which point the spectrum magnitude has only decayed 10 to 20 dB. Also, single impacts must be insured, as double and multiple hits cannot be used since the spectrum will contain zeros with a spacing of  $n/t_r$ ,  $n$  being the and integer and  $t_r$  the time delay between dual impacts. This is best described in figure 22. Due to our system being

a fragile one, and since we want to cover a frequency range of relatively high frequencies, we use for this test a miniature hammer, weighing 4,8 grams, with a silicone head minimizing the chance of damage to the instrument. The measured force is the mass of the impactor behind the piezoelectric disc of the force transducer, multiplied by the acceleration. The true force that excites the structure, is equal to the total mass of the impactor multiplied by the acceleration during the impact. The true force is the measured force multiplied by the ratio of total mass/the mass behind the transducer piezoelectric.

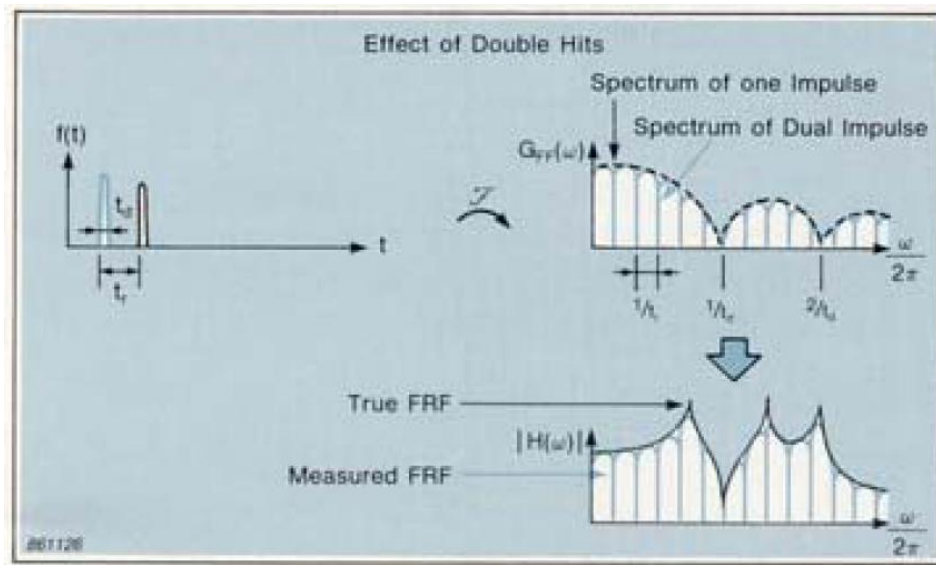


**Figure 22** Effect of double hits (Døssing, 1988b)

An impact test has been chosen over a shaker test as, while there is theoretically no difference between them (Avitabile, 2001), practical aspects become relevant, such as the fact that in this study we do not want any vibrations interfering with the system besides the vibration treatment, and that the mass and stiffness effect of shaker attachment may affect the modes of the structure.

In response to the force exerted by impact, three accelerometers, two placed in the top plate, and one place in the back plate, will send an electric signal, passing through our pre-amplifiers which increase the voltage signals, which are then digitalized and recorded by the digital acquisition card. The pre-amplifiers must be set for the accelerometers sensitivities, which have been determined by previous calibration. When digitalizing the signals several precautions must be taken, including using the correct sampling frequency in accordance to Shannon's Theorem (Taub & Schilling, 1986).

The guitar top plate has been meshed in 178 points. The use of this number of measure points is justified to create a full identification, including the geometry of the mode shapes of the structure. In other words we want, not only to predict modal frequencies, but to construct a mathematical model that describe the complex mode shapes of the structure. These measurement points correspond to the points where hammer impacts have been applied and corresponding inputs recorded. The top plate accelerometers were placed in points 76 and 154, as can be seen in figure 23. They were mounted with the use of bee wax, as is it a non-damaging way of connecting the accelerometers to the guitar. Due to the linearity assumption, we will have an implication described as the Reciprocity Theorem (Døssing, 1988b): the FRF measured between any two measure points is independent of which of them measures input or output. This justifies, that for practical reasons, hammer impacts are performed in all measure points, keeping the accelerometers fixed in the same points, as the result would be the same as impacting one point and moving the accelerometers from point to point.

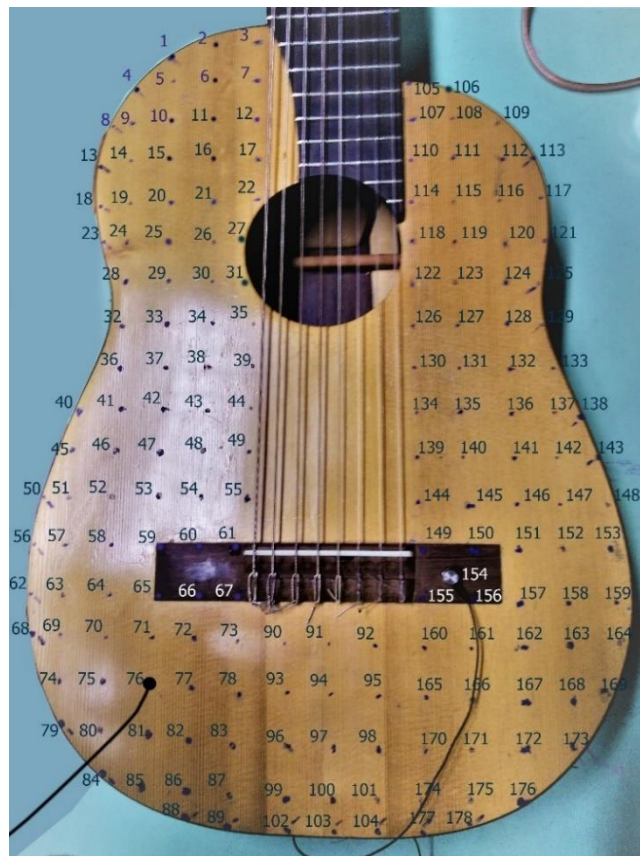


**Figure 23** The tested guitar with the mesh of measurement points

Other implications are superposition, meaning that a measured FRF is not dependant on the type of excitation used, and homogeneity meaning a measured FRF is independent of the excitation level (Døssing, 1988b).

### 3.3.2.1. Results

Making use of an impact hammer and an accelerometer on the guitar system, the signals have been recorded and digitized by an acquisition board, which performs Fast Fourier Transforms, to obtain the FRF. We acquired the FRF of the guitar with a bandwidth of 2 kHz with a frequency resolution of 0.625Hz. In figure 24, it is possible to observe the experimental hammer input in the time domain and the FRF. This data is then processed using our developed software with the implementation of the ERA. In figure 25, we can observe the FRF backed with a stabilisation diagram that accounts for the identified natural frequencies and corresponding modal damping. We select the minimum model order to which the real modal frequencies have all stabilized, as observed in figure 25 by the dotted line.

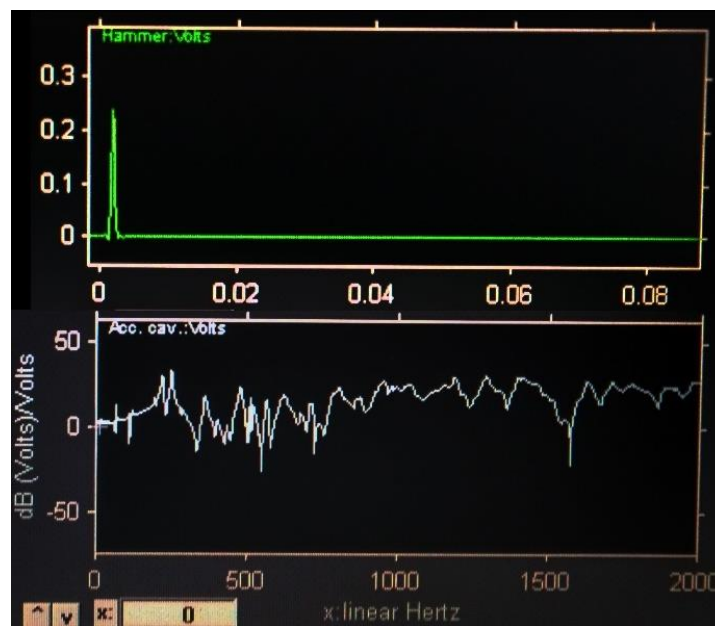


Figure 24 Experimentally obtained input impulse and FRF

Our next step is to select the real modal parameters discarding the computation parameters. In the developed software, as seen in figure 26, this selection is made by

observing a counting of the number of times a determined frequency has been identified by ERA in increasing model order to the maximum selected model order.

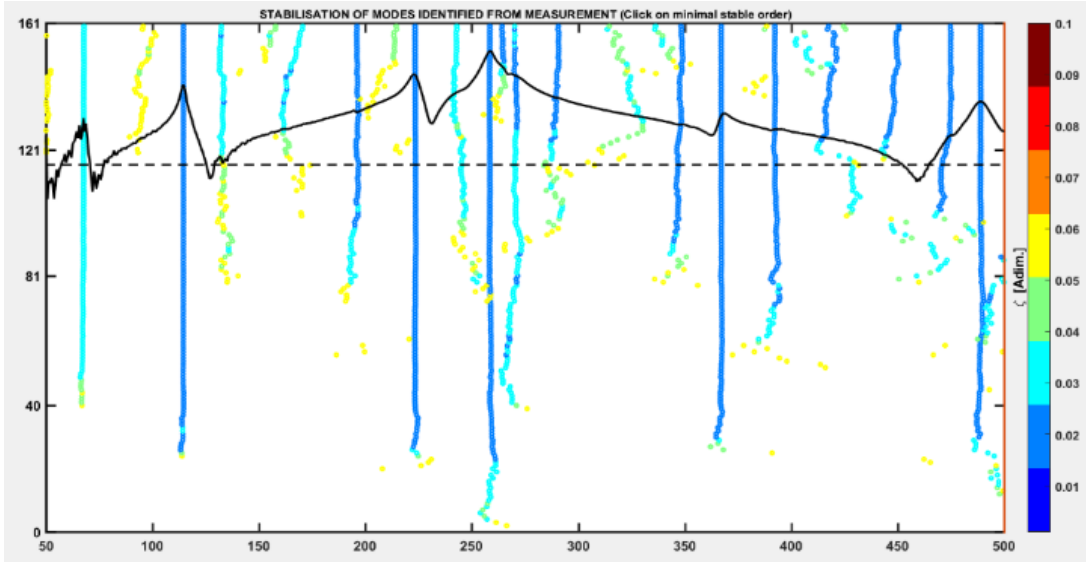


Figure 25 FRF with stability diagram

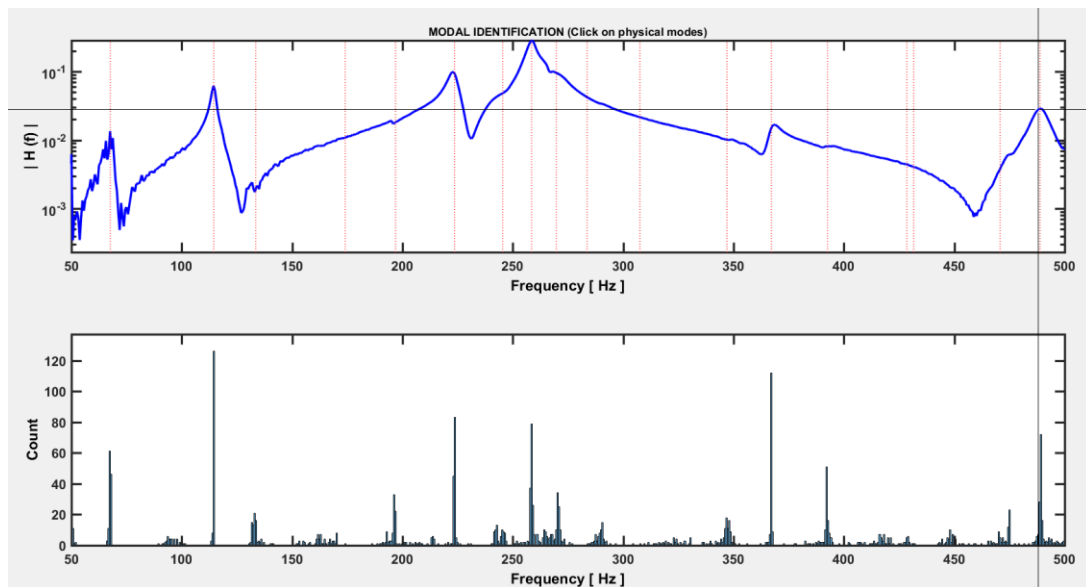


Figure 26 Selection of the real modal parameters

Being the nonphysical modal parameters discarded, the software presents the correct identification of the real parameters.

With a basis on the ERA formulation the software then computes the mode shapes for all the identified modes. In table 2 are presented the values of the modal identification performed before the treatment.

| Modes | $f_n$ [Hz] | $\zeta_n$ [%] | $\varphi$ |
|-------|------------|---------------|-----------|
| 1     | 67.7       | 1.82          | Bending   |
| 2     | 114.5      | 0.97          | (0,0)     |
| 3     | 223.6      | 1.01          | (0,0)     |
| 4     | 258.5      | 1.03          | (1,0)     |
| 5     | 367.1      | 0.70          | (0,1)     |
| 6     | 488.9      | 0.66          | (2,1)     |

**Table 2** Modal parameters before treatment

With our identified modal parameters, it is possible to plot our identified impulse response function as seen in equation (3.16). We compare it to the measured impulse response to observe if our identified parameters are accurate enough to reproduce a function close to the measured one. The same has been done to the transfer function. The resulting functions are seen in figure 27, which leads us to believe in the accuracy of our results.

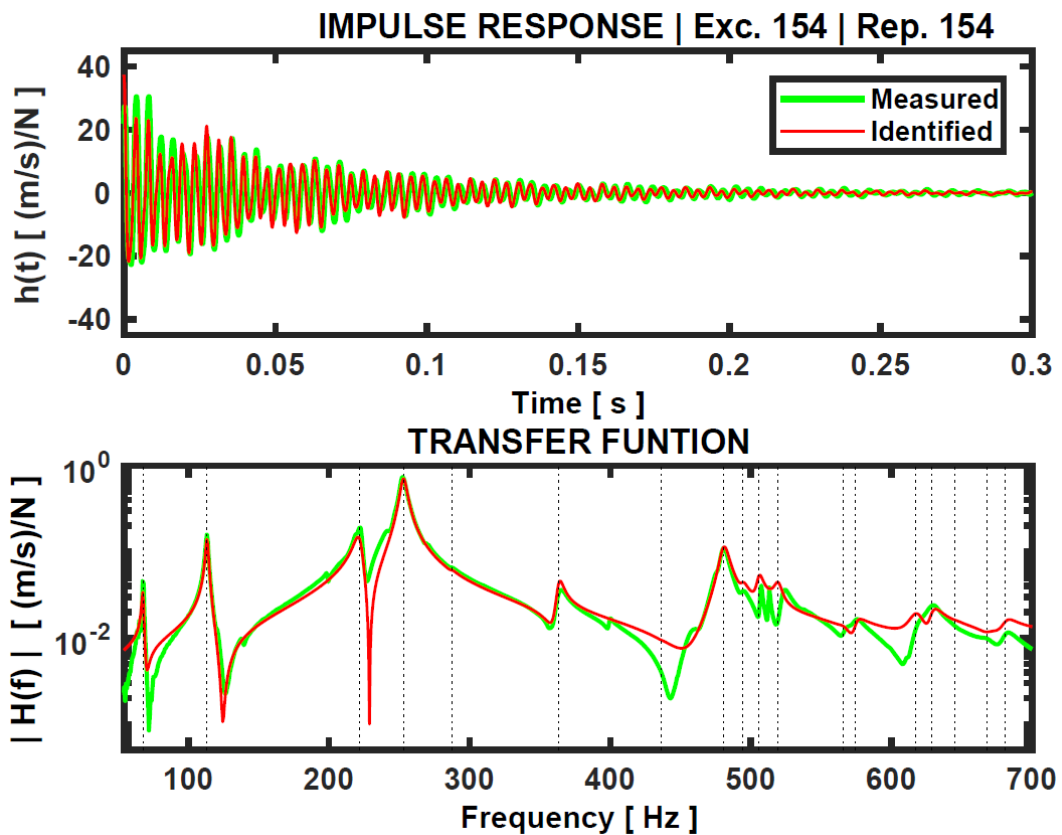


**Figure 27** Comparison between the measured and identified impulse response and transfer function

We proceed to singularly evaluate the identified modes in comparison to the available literature.

### 3.3.2.2. First Mode – Bending mode

The first mode identified sits at the natural frequency of 67.7 Hz, with a modal damping of 1.82% and the mode shape, as seen in figure 28, shows a full bending of body with the nodal line probably between the body and the neck. An equivalent bending mode is described in literature (Van Karsen, 1997), with the same mode shape at 65.5 Hz with a damping of 0.708.

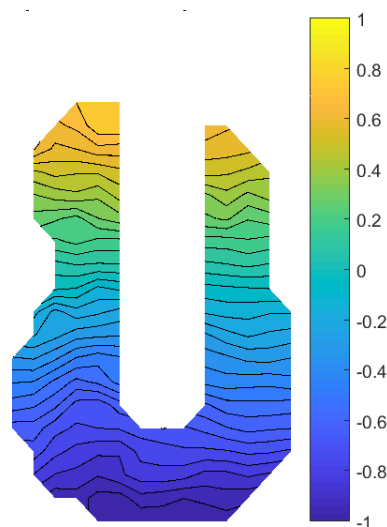


Figure 28 First mode shape of the guitar

### 3.3.2.3. Second and Third Mode (0,0) – Breathing Modes

The second and third identified modes are, as literature indicates (Christensen, 1984; Elejabarrieta et al., 2002; Rossing, 2010; Van Karsen, 1997), what is called the breathing modes, as they result from the coupling of the plate modes and air modes, creating a “breathing” movement of the guitar. The mode shapes can be seen in figure 29 and are found to be at 114,5 Hz and 223.6 Hz, with modal damping of 0.97% and 1.01% respectively. This goes according to literature (Christensen, 1984; Elejabarrieta et al., 2002; Rossing, 2010; Van Karsen, 1997) that situates these modes usually around 100 Hz for the first breathing mode and at 200 Hz for the second breathing mode. The geometrical index we are using  $(y,x)$  is relative to the number of nodal lines in the vertical and horizontal direction.

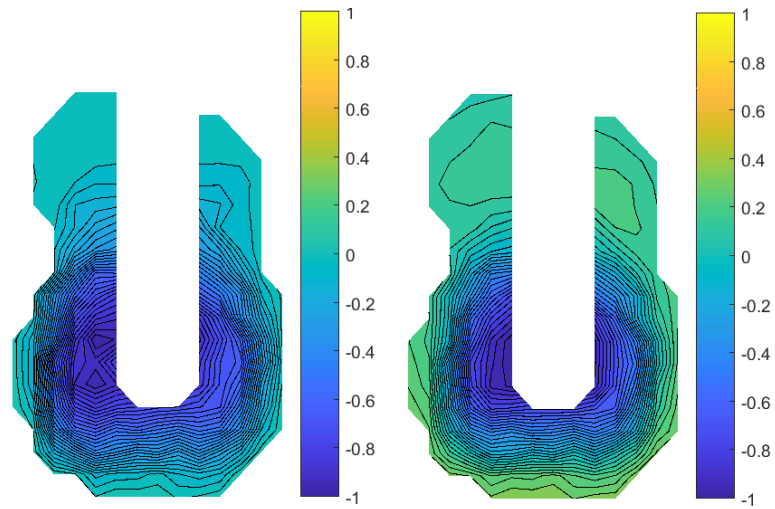


Figure 29 Second and third mode shapes

#### 3.3.2.4. Fourth Mode (1,0)

The fourth identified mode is found at 258.5 Hz with a modal damping of 1.03%, with a mode shape (0,1) as shown in figure 30. This mode goes according to literature (Christensen, 1984; Rossing, 2010; Van Karsen, 1997) that places this mode to be found after the breathing modes at around 250 Hz to 300 Hz.

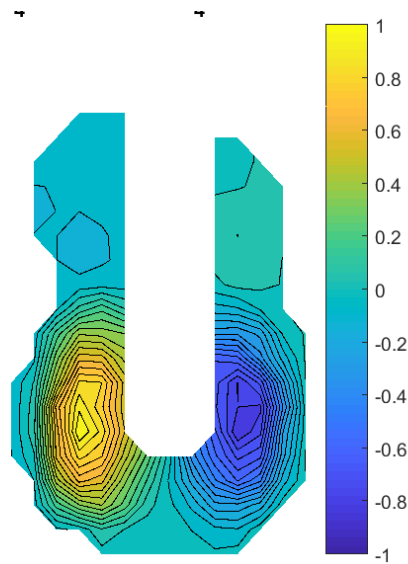


Figure 30 Fourth identified mode shape

### 3.3.2.5. Fifth Mode (0,1)

The fifth mode was identified at 367.1 Hz with a modal damping of 0.7%. The mode shape is shown in figure 31. This is also according to literature (Christensen, 1984; Elejabarrieta et al., 2002), that places this mode after the (1,0) mode and around 300 to 400 Hz.

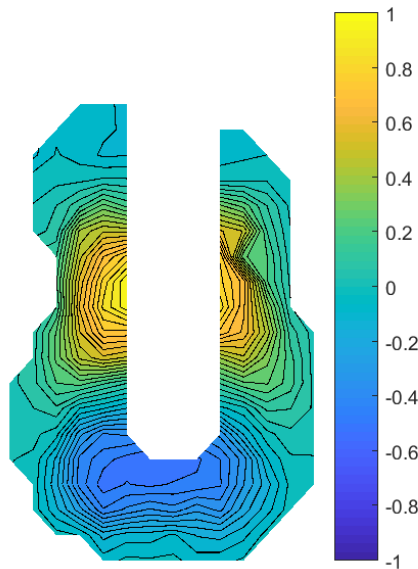


Figure 31 Fifth identified mode shape

### 3.3.2.6. Sixth mode (2,1)

The sixth mode is found at the natural frequency of 488.9 Hz with a modal damping of 0.66%. The mode shape is shown in figure 32. This mode is also according to literature (Christensen, 1984; Elejabarrieta et al., 2002) that places this mode after the (0,1) mode, and is found to be between 300 and 600 Hz.

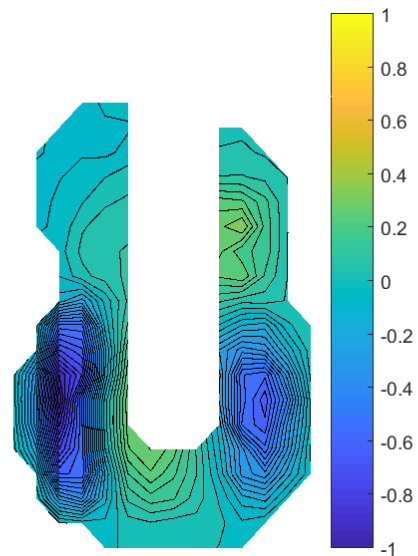


Figure 32 Sixth identified mode shape

## 4. VIBRATION TREATMENT

We intended to design a vibration treatment that would resemble the most the vibrations induced during regular practice and play of musicians. To do so, we recorded the actual playing vibration of a guitar through an accelerometer. Then, by solving the inverse problem, we identified a voltage signal that, sent to a shaker device, will accurately reproduce on the guitar the vibrations felt during playing. In this chapter we present the development of our method, from the construction of the problem to the system developed to induce vibration in our guitar.

### 4.1. Inverse Problem

In the experimental set-up, a shaker will be used to induce the vibrations in the guitar top plate. For its use, a tension input is sent to the shaker which converts the signal into mechanical vibration. We want this mechanical vibration to closely simulate the vibrations transferred to the top plate by the strings being played. Our equation for the FRF becomes:

$$\ddot{X}(\omega) = V(\omega)H(\omega) \quad (4.1)$$

where  $H(\omega)$  is the electro-mechanical transfer function obtained experimentally for the system,  $V(\omega)$  is the voltage to be sent to the shaker and  $\ddot{X}(\omega)$  is the acceleration measured on the top plate during playing.

Using an accelerometer, we recorded the acceleration felt in the guitar's saddle with Professor Paulo Vaz de Carvalho playing parts of classical pieces and musical scales. This makes up for the  $\ddot{X}(\omega)$  part of the equation. We want to determine  $V(\omega)$  and this makes up for the inverse problem:

$$V(\omega) = H(\omega)^{-1}\ddot{X}(\omega) \quad (4.2)$$

An inverse problem is when it is intended to find the cause of an observed effect. The observed effect being the acceleration on the top plate and the cause being the voltage sent to the shaker. It is then needed to solve the inverse problem:

For the linear system

$$Ax = b \quad (4.3)$$

Being  $A$  an  $m \times n$  matrix, the rank of  $A$  determines the nature of the solution, which can be unique, overdetermined (with no solution) or with more than one solution. The system always has a least squares solution, and a unique generalized solution. If the rank is unknown it is not trivial to determine it.

We stand, in our case, before an equation with multiple solutions. To help solve this kind of problems it is desirable to inject in the process the concept of plausibility, based on what is expected of the solution.

Suppose that the exact solution  $x$  of equation (4.3) is known. It is possible to compute the residual:

$$\rho(x) = Ax - b \quad (4.4)$$

Because of the rounding that happens in computations, even the exact solution will not produce a zero residual. This means it is not possible to distinguish between an exact solution  $x$  from an approximation  $\hat{x}$ , and in practical terms both must be considered possible solutions. For a badly conditioned  $A$  this means many possible and very different solutions exist. Because of this uncertainty in the solution of the ill-conditioned system, we must use our expectations of the true solution, constraining solutions to eliminate those which are considered undesirable. This is what is called regularization.

One way to regularize an ill-conditioned linear system is to use the method of *Singular Value Decomposition (SVD) with cut-off*. Supposing all computational errors can be accounted for by adding term  $\Delta b$ , the computed solution  $\hat{x}$  of (4.3) stands as:

$$A\hat{x} = b + \Delta b \quad (4.5)$$

The unique generalized solution is:

$$\hat{x} = \sum_{i=1}^n \frac{1}{\lambda_i} v_i^T (b + \Delta b) u_i \quad (4.6)$$

So

$$\hat{x} - x = \sum_{i=1}^n \frac{1}{\lambda_i} v_i^T \Delta b u_i \quad (4.7)$$

This means that small errors  $\Delta b$  are magnified for small singular values, resulting in large errors in the computed solution. The method suggests that computational errors effects can be limited by choosing a cut-off level  $\alpha$  and dropping terms for which  $\lambda_i < \alpha$ . This method however is flawed as the choice of  $\alpha$  can have a major effect on the solution.

For our study we use the method of Water Level Regularization. We must take into consideration that this is an inverse problem and that our transfer function  $H(\omega)$  is measured experimentally. This means that we'll have noise, which is undesirable data, at frequencies where  $H(\omega)$  has a small value. What the water level regularization does (Aster, Borchers, & Thurber, 2005) is, for a critical level  $\varepsilon$ ,  $H(\omega)$  is adjusted if  $|H(\omega)| < \varepsilon$ . This regularization states that the regularized  $H(\omega) = \hat{H}(\omega)$ :

$$\hat{H}(\omega) = \begin{cases} H(\omega), & \text{for } H(\omega) > \varepsilon \\ \varepsilon \frac{H(\omega)}{|H(\omega)|}, & \text{for } 0 < H(\omega) < \varepsilon \\ \varepsilon, & \text{for } H(\omega) = 0 \end{cases} \quad (4.8)$$

What is critical about this, is the optimal choice of  $\varepsilon$ . For this the L-Curve Method has been used (Aster et al., 2005; Hansen, 2000). As seen in equation (4.4), we want to minimize the residual. Equation (4.4) takes the form:

$$\rho(x) = \left\| H(\omega)V(\omega) - \ddot{X}(\omega) \right\| \quad (4.9)$$

The values of  $\rho(x)$  for various values of  $\varepsilon$  are computed, and so as the resulting  $V(\omega)$ . We find that the results for small  $\varepsilon$ , the residual will be closer to zero, but the resulting  $\hat{H}(\omega)$  will be deficiently regularized and  $V(\omega)$  will be largely amplified. On the contrary, for large  $\varepsilon$ , the residual will be large, and the resulting  $\hat{H}(\omega)$  over-regularized. According to the L-curve method, the critical value of  $\varepsilon$  can be identified plotting the residual against the norm, on a logarithmic scale. This will create an L-shaped curve with a sharp corner which contains the critical value, as seen in figure 33.

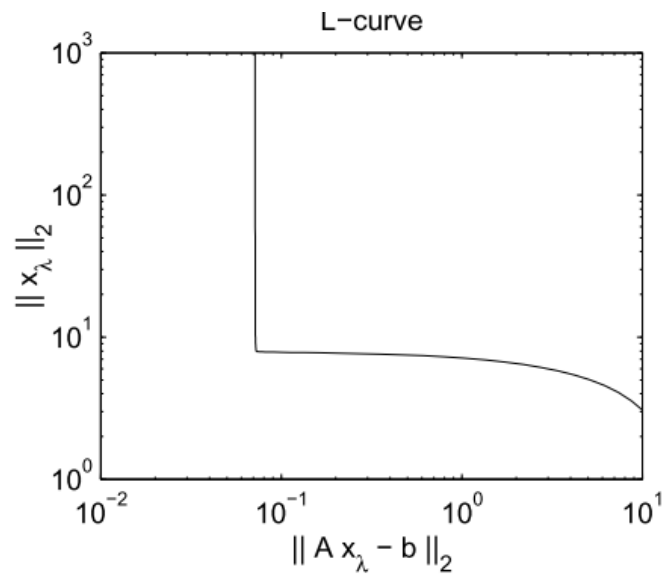


**Figure 33** Typical L-Curve (Hansen, 2000)

## 4.2. Experimental Set-up

### 4.2.1. Recording acceleration

The first step to create our vibration treatment which relies on the inverse problem described, is to record the acceleration  $\ddot{X}(\omega)$  that occurs in the guitar top plate. As seen in figure 34, we asked Professor Paulo Vaz de Carvalho to play classical pieces and scales while recording the acceleration with the aid of an accelerometer in measure point 154 with a bandwidth of 20kHz. The signal is then passed through a properly set pre-amplifier and digitalized by the Digital acquisition card in the time domain, recording it on the PC.



**Figure 34** Professor Paulo Vaz de Carvalho recording of playing acceleration

#### 4.2.2. Measuring transfer-function and vibration set-up

A complete diagram of the experimental set-up can be observed on figure 35.

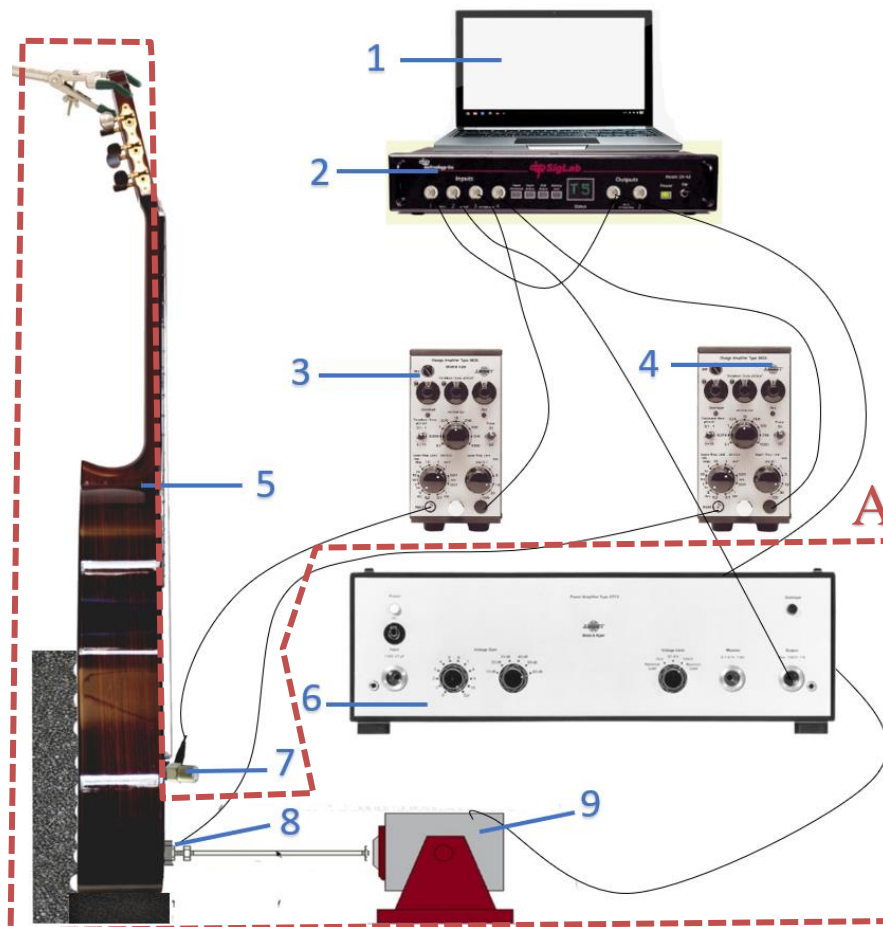


Figure 35 Experimental set-up for determining the transfer function

On this set-up we have: (1) Laptop with acquisition software; (2) Digital acquisition card (Spectral Dynamics model 20-42); (3)-(4) *Bruel & Kjaer* type 2635 Pre-amplifiers; (5) Guitar; (6) *Bruel & Kjaer* type 2713 Power Amplifier; (7) Accelerometer placed in measure point 154; (8) Force transducer; (9) Shaker with stinger attachment.

The next step in our vibration treatment, so that we can resolve the inverse problem, is to use the correct transfer function  $H(\omega)$ . We observe that the  $H(\omega)$  obtained previously in our experimental modal analysis can no longer be used since the experimental set-up has changed, coupling the guitar with the shaker system, and introducing a power amplifier. A new electro-mechanical  $H(\omega)$  must be obtained for the new system which is done by means of a frequency sweep. This is an alternative mode to the impact testing for obtaining the transfer function. Once again, the definition of the Frequency Response Function is used. A sweep function, with specific parameters controlled on the Siglab

software, is sent from the digital card into the power amplifier and into the shaker. The shaker excites the structure progressively from the low-end frequencies to the highest frequencies. This will create a response on the guitar which is the output measured by the accelerometer. The input will no longer be the force exerted but rather the voltage input by the digital acquisition card. This way the measured  $H(\omega)$  is for the system contained inside the “A” group as seen in figure 34. This way, the resolution of the inverse problem will give us the voltage input that is to be sent from the digital card. This voltage input, resulting from the inverse problem, will make the shaker excite the top-plate in a way that it will be equivalent to the acceleration originally recorded. This will allow to continuously excite the guitar, to simulate long-term playing of the instrument, and analyse this evolution on the modal parameters.

To analyse the evolution of the transfer function of the guitar, without disassembling the vibration treatment experimental set-up, we use the signals captured by the force transducer and accelerometer to create the transfer function of the guitar body.

Our experimental set-up is presented in figure 36 and 37.



**Figure 36** Experimental set-up for vibration treatment

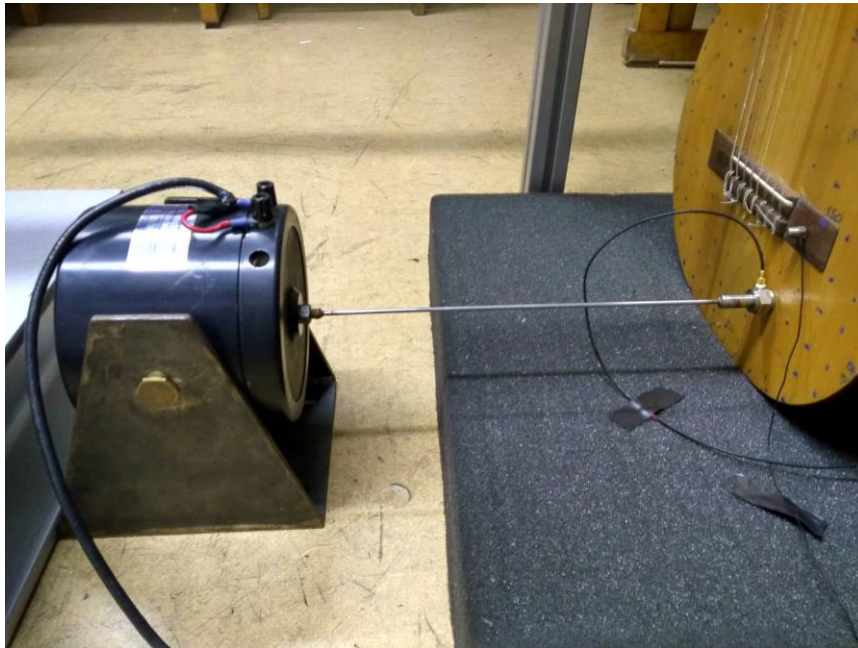


**Figure 37** Detail of the shaker and accelerometer from the experimental-setup for vibration treatment

### 4.3. Results

With the experimentally measured  $H(\omega)$  we begin by applying our Water Level method of regularization. The critical level  $\varepsilon$  is chosen by plotting the residual and solution semi norm for a series of values  $\varepsilon$ , which form the L-Curve, as seen in figure 38, and applied to our transfer function, as seen in figure 39.

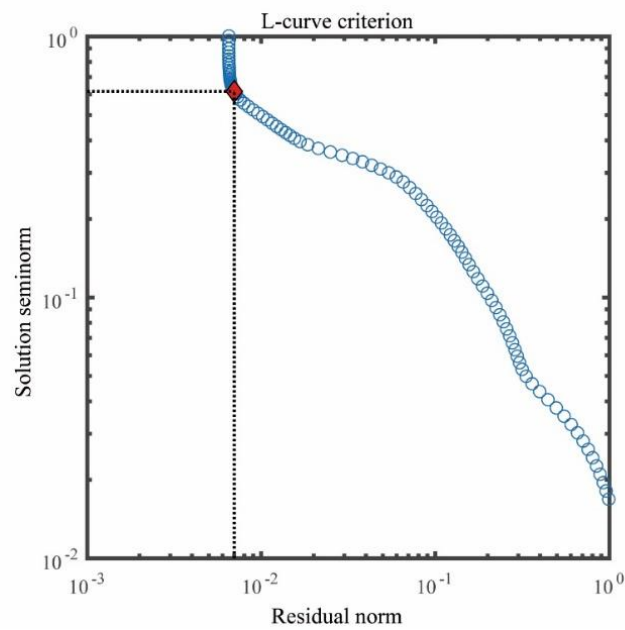


**Figure 38** Plotted L-Curve

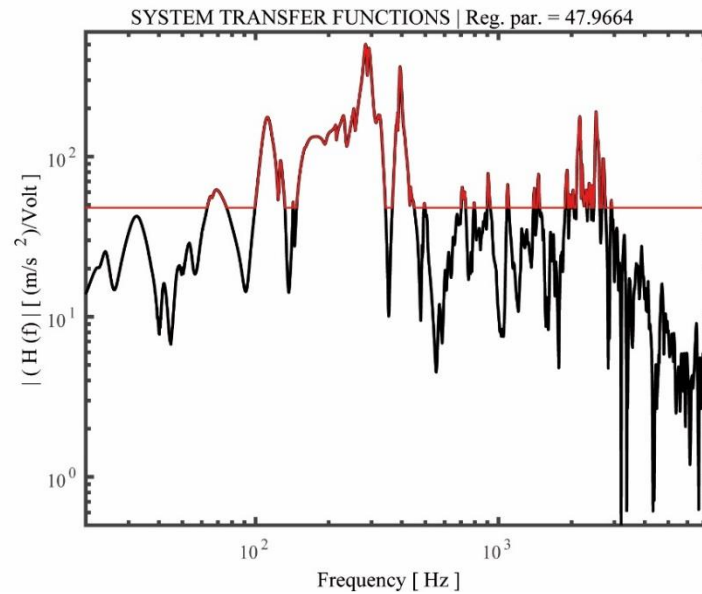


**Figure 39** Application of the critical level

As observed the critical level used keeps our peaks of information intact while removing the anti-resonances and the noise from the lower points. Using the regularized  $\hat{H}(\omega)$  we can solve the inverse problem to obtain our voltage. The measured acceleration for a played part of the classical piece “Asturias” by composer *Isaac Albeniz* is plotted in figure 40, as well as the identified voltage obtained from the inverse problem. We can observe that the signals, while similar, are different between themselves.

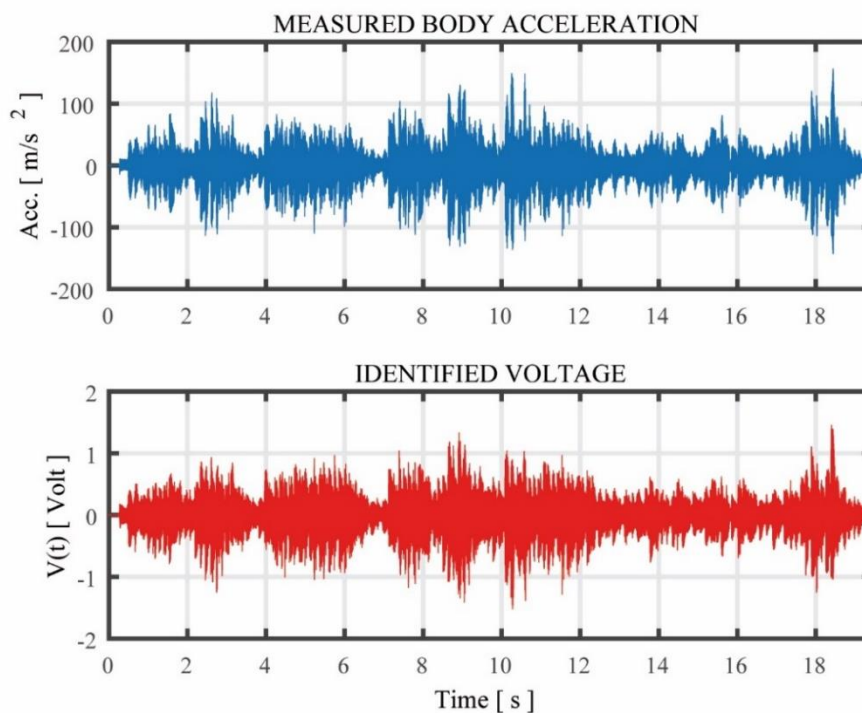


**Figure 40** Measured acceleration and corresponding identified voltage

To test the accuracy of our results, we measured the acceleration felt by the accelerometer when the identified voltage is sent to the shaker and compared it with the original acceleration felt when the guitar is being played, measured at the same point. This comparison is shown in figure 41 and 42, making it possible to conclude that the artificial vibration emulates with proximity the vibration of the guitar being played. The differences observed are expected as they are a consequence of the regularization.

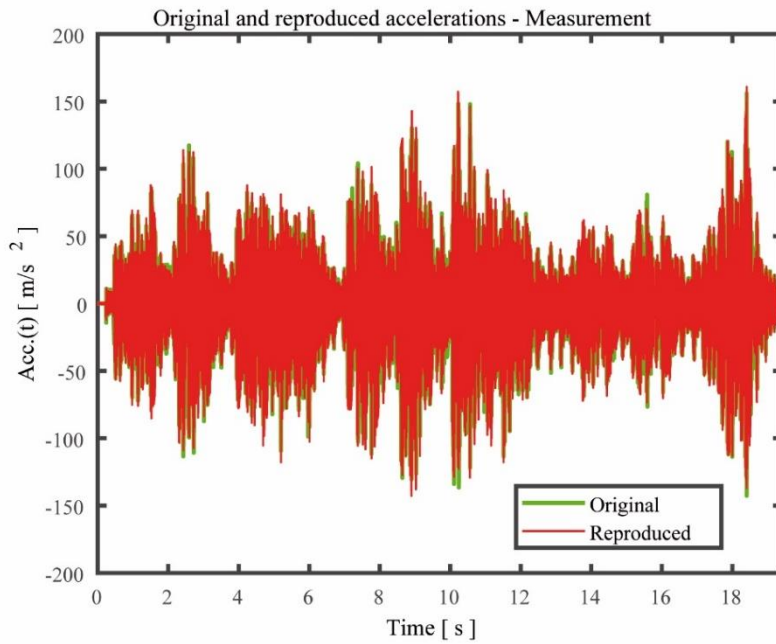


**Figure 41** Comparison between the original acceleration signal and the one reproduced

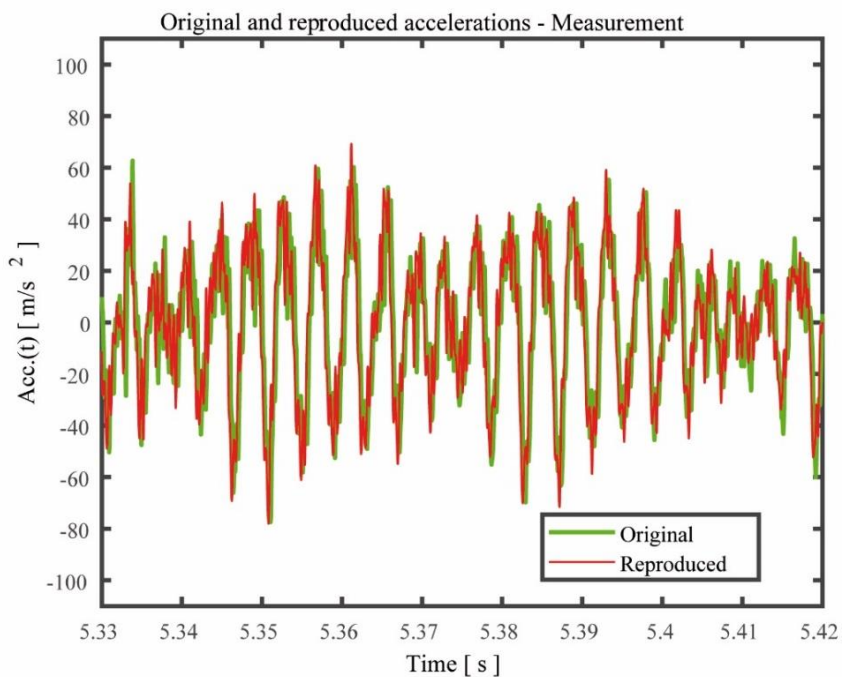


**Figure 42** Zoomed in comparison between original and reproduced acceleration

## 5. EXPERIMENTAL PROTOCOL

The experiment is preceded and finalized by a free-boundary condition experimental modal analysis, as described in the modal identification experimental set-up, to compare the full evolution of the guitar system between the start and finish of the vibration treatments. After the initial modal analysis, we mount the experimental set-up for the vibration treatments. This set-up will not be changed for the duration of the vibration treatments. A sweep is made, as described in 5.2.2., and used to create the voltage signal to be sent to the shaker. For the duration of the days of vibration treatment the following method is applied daily:

1. Tuning of the guitar to keep string tension constant.
2. Obtaining transfer function with the sinusoidal sweep, registering the time, temperate and room humidity for control.
3. Applying the vibration treatment, registering number of daily hours, temperature and humidity conditions at the beginning and end of the treatment.
4. Obtaining the transfer function in similarity to step 2. at the end of the treatment.

Comparing the evolution of the transfer functions and, in case of modification of the transfer function, using it to create a new voltage signal to be sent to the shaker.



## 6. TREATMENT AND RESULTS

### 6.1. Applied treatment

The treatments for this project have been applied for a duration of 12 days, with the following characteristics of initial and final temperature and humidity, and hours of excitation.

| Day | $T_i, H_i$ | $T_f, H_f$ | Duration of the excitation |
|-----|------------|------------|----------------------------|
| 1   | 28°C , 45% | 28°C , 46% | 2h                         |
| 2   | 27°C , 51% | 28°C , 50% | 7h                         |
| 3   | 27°C , 45% | 28°C , 43% | 7h                         |
| 4   | 26°C , 44% | 27°C , 45% | 6h20                       |
| 5   | 26°C , 44% | 27°C , 44% | 6h                         |
| 6   | 27°C , 45% | 28°C , 46% | 4h                         |
| 7   | 27°C , 49% | 27°C , 48% | 7h                         |
| 8   | 27°C , 55% | 26°C , 57% | 6h                         |
| 9   | 26°C , 53% | 25°C , 52% | 7h20                       |
| 10  | 24°C , 53% | 26°C , 52% | 7h20                       |
| 11  | 25°C , 52% | 25°C , 52% | 7h30                       |
| 12  | 25°C , 52% | 26°C , 53% | 3h30                       |

**Table 3** Applied treatments

This totalizes in 71 hours of continuous treatment with a maximum temperature amplitude of  $\pm 2^\circ\text{C}$  and maximum relative humidity amplitude of  $\pm 7\%$ . For reference Barclay (1997) states that for historical instruments the benefits of preserving an instrument at relative humidity  $\pm 5\%$  or higher are indistinguishable.

### 6.2. Preliminary Results

After 12 days of treatment, a new modal identification of the guitar has been performed, setting the instrument in the original free-boundary condition experimental set-up. In figure 43, we can observe a comparison between the transfer functions, measured at

point 154, before and after the vibration treatment. The red line corresponds to the transfer function measured before the vibration treatment and the blue line corresponds to the transfer function measured after the vibration treatment.

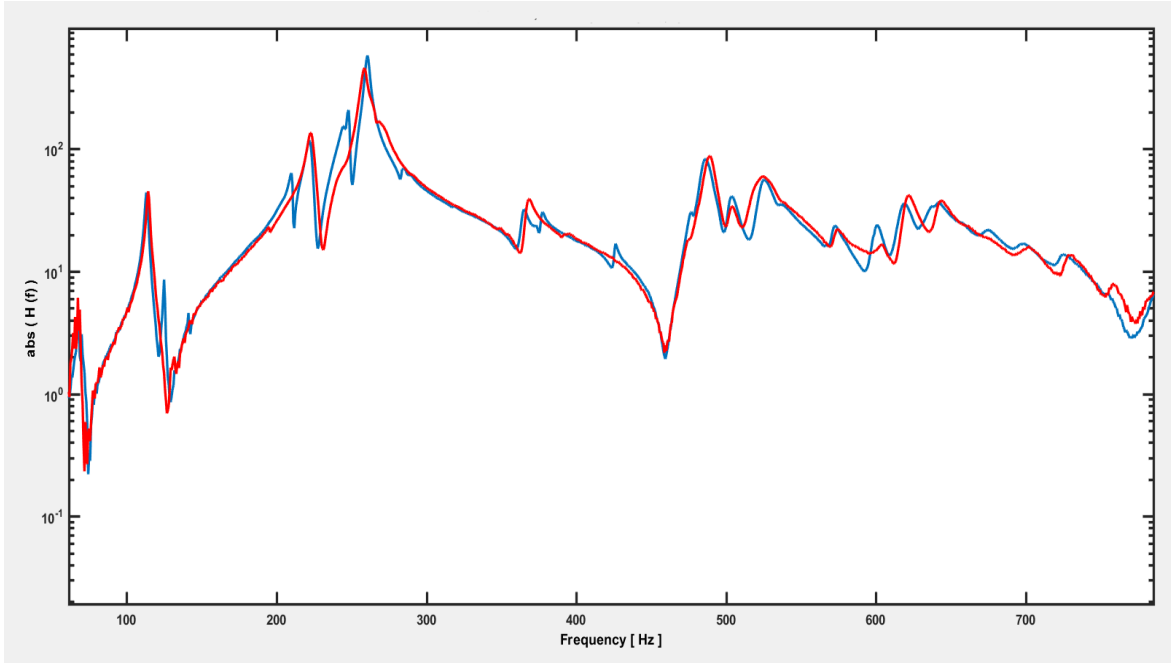


Figure 43 Transfer function comparison

Preliminary observation reveals slight changes in the vibratory response of the guitar before and after the treatment. In figure 44 we can observe that the natural frequency at around 260Hz appears to be less damped, and some previously irresponsive modes around 245Hz seem to be “activated”.

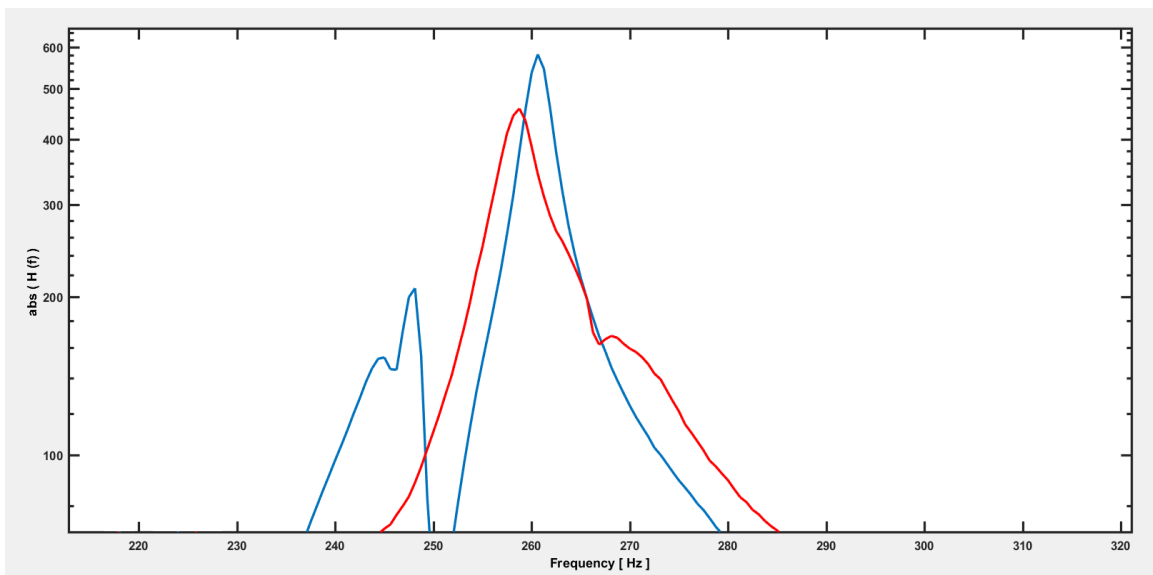


Figure 44 Transfer function comparison zoom on the 260Hz mode

To provide quantitative data, we proceed to apply modal identification with the ERA technique and compare the results before and after the treatment, for 2 response locations, as presented on tables 4 and 5.

| Measure point 154 |           |               |           |                 |               |           |                 |        |
|-------------------|-----------|---------------|-----------|-----------------|---------------|-----------|-----------------|--------|
| Before Treatment  |           |               |           | After Treatment |               |           | $\Delta\zeta_n$ |        |
| Modes             | $f_n[Hz]$ | $\zeta_n[\%]$ | $\varphi$ | $f_n[Hz]$       | $\zeta_n[\%]$ | $\varphi$ | Total           | [%]    |
| 1                 | 67.7      | 1.82          | Bending   | 67.6            | 1.33          | Bending   | -0.49           | -26.9% |
| 2                 | 114.5     | 0.97          | (0,0)     | 113.3           | 0.85          | (0,0)     | -0.12           | -12.4% |
| 3                 | 223.6     | 1.01          | (0,0)     | 222.5           | 0.92          | (0,0)     | -0.09           | -8.9%  |
| 4                 | 258.5     | 1.03          | (1,0)     | 260.5           | 0.59          | (1,0)     | -0.44           | -42.7% |
| 5                 | 367.1     | 0.70          | (0,1)     | 364.1           | 0.69          | (0,1)     | -0.01           | -1.4%  |
| 6                 | 488.9     | 0.66          | (2,1)     | 485.6           | 0.7           | (2,1)     | +0.04           | +6.1%  |

Table 4 Evolution of modal identification parameters in point 154

| Measure point 130 |           |               |           |                 |               |           |                 |        |
|-------------------|-----------|---------------|-----------|-----------------|---------------|-----------|-----------------|--------|
| Before Treatment  |           |               |           | After Treatment |               |           | $\Delta\zeta_n$ |        |
| Modes             | $f_n[Hz]$ | $\zeta_n[\%]$ | $\varphi$ | $f_n[Hz]$       | $\zeta_n[\%]$ | $\varphi$ | Total           | [%]    |
| 1                 | -         | -             | -         | -               | -             | -         | -               | -      |
| 2                 | 114.5     | 0.98          | (0,0)     | 113.3           | 0.86          | (0,0)     | -0.12           | -12.2% |
| 3                 | 223.5     | 1.00          | (0,0)     | 222.4           | 0.99          | (0,0)     | -0.01           | -1%    |
| 4                 | 258.5     | 0.95          | (1,0)     | 260.5           | 0.57          | (1,0)     | -0.38           | -40%   |
| 5                 | 366.8     | 0.70          | (0,1)     | 364.0           | 0.75          | (0,1)     | +0.05           | +7.1%  |
| 6                 | 489       | 0.66          | (2,1)     | 486.0           | 0.81          | (2,1)     | +0.15           | +22.7% |

Table 5 Evolution of modal identification parameters in point 130

Both identifications show consistent values and consistent variations of modal damping for the first predominant three modes (modes 2-4). The decrease in modal damping of the 4<sup>th</sup> mode is about 40%, which is of significant value. However, the acoustical consequences of a change in the modal parameters for this mode are certainly limited, because of the symmetry of the corresponding mode shapes, which favours an acoustic short-circuit. Surprisingly, several new modes have been identified, at approximately 125 Hz, 210 Hz, 249 Hz and 425 Hz, and this brings more data into this long-term study, which needs careful investigation (for instance by performing a full modal analysis of the treated instrument). Nevertheless, it is important to stress that 12 days of treatment is relatively short, and is certainly less than what we can call regular guitar playing. This study will continue, and more hours of vibration treatment will be performed during the next weeks.

However, an important aspect for the continuation of the project, is to account for the observed changes and, in particular, to adapt the signals to be sent to the guitar in order to account for the changes of the whole system dynamics.

## 7. CONCLUSIONS

We intended to study the effects that playing vibrations had on the vibrational qualities of modern classical guitars. To do so we developed a mechanical set-up for vibration treatment that could simulate playing and used experimental modal analysis to follow the evolution of the vibrational characteristics of the guitar with excitation time.

The development of the vibration treatment and system has been highly successful, accurately reproducing the acceleration felt by the guitar when being played, allowing for a whole set of future multipurpose studies in guitars and stringed instruments in general.

In its present time, a preliminary analysis of the results by modal analysis shows some slight changes in the vibratory response of the guitar. The damping of one low-frequency mode has decreased notably, and some modes seem to have been activated after 12 days of vibration treatment.

Several issues are raised by these observations. What are the corresponding mode shapes of the newly activated modes? Were they highly damped in the original guitar and therefore not identified in our original modal identification? Does the coupling between different parts of the instrument have changed? Are these modes acoustically important? Why has the damping of a single mode changed? Does this come from changes in the guitar behaviour or in the wood properties? To address all these questions, further investigation is needed, and a full modal identification of the treated guitar will soon be performed.

Because our study deals with the vibrational behaviour of the guitar, it is not possible to make conclusions about the improvement of the guitar sound. Further studies could determine the level of sound radiation that comes from the mode that suffered damping reduction, to learn more about its influence on sound. Also, the change in the modal parameters must be observed for a longer time of excitation in order to determine if the evolution is consistent.

This study will continue, and the vibration treatment will be applied for a longer period of time. Our results will soon be presented at the conference TECNIACUSTICA'18 - XI Congreso Iberoamericano de Acústica, in Cádiz, Spain



---

## BIBLIOGRAPHY

- Akahoshi, H., Chen, S., & Obataya, E. (2005). Effects of Continuous Vibration on the Dynamic Viscoelastic Properties of Wood. *COST FP1302 WOODMUSICK Conference Guide and Abstracts*, 43–44. Retrieved from <http://hdl.handle.net/2241/00143998>
- Aster, R. C., Borchers, B., & Thurber, C. H. (2005). *Parameter Estimation and Inverse Problems*. Elsevier Academic Press.
- Avitabile, P. (2001). Experimental Modal Analysis: A Simple Non-Mathematical Presentation. *Sound and Vibration*, (January), 1–11.  
<https://doi.org/10.1016/j.jbiomech.2011.03.005>
- Barclay, R. L. (1997). *The Care of Historic Musical Instruments*. Edinburgh: Canadian Conservation Institute and the Museums & Gallery Commission.
- Bretos, J., Santamaría, C., & Moral, J. A. (1999). Vibrational patterns and frequency responses of the free plates and box of a violin obtained by finite element analysis. *The Journal of the Acoustical Society of America*, 105(3), 1942–1950.  
<https://doi.org/10.1121/1.426729>
- Brown, D. L., Allemang, R. J., Zimmerman, R., & Mergeay, M. (1979). Parameter estimation techniques for modal analysis. *SAE Technical Paper Series*, (No. 790221).
- Bucur, V. (2016). *Handbook of Materials for String Musical Instruments*.  
<https://doi.org/10.1007/978-3-319-32080-9>
- Chanan, M. (1994). *usica Practica: The Social Practice of Western Music from Gregorian Chant to Postmodernism*.
- Christensen, O. (1984). An Oscillator Model for Analysis of Guitar Sound Pressure Response. *Acustica*, 54, 289–295.
- Clemens, B. M., Adis, J. K., Clemens, D. M., Ollak, E. P., Lark, P. C., & Roves, J. R. G. (2014). Effect of Vibration Treatment on Guitar Tone : A Comparative Study. *Savart Journal*, 1–9.
- Døssing, O. (1988a). Structural Testing Part I: Mechanical Mobility Measurements. Brüel & Kjær.

- Døssing, O. (1988b). Structural Testing Part II : Modal Analysis and Simulation. Brüel & Kjør.
- Elejabarrieta, M. J., Ezcurra, A., & Santamaría, C. (2002). Coupled modes of the resonance box of the guitar. *The Journal of the Acoustical Society of America*, *111*(5), 2283. <https://doi.org/10.1121/1.1470163>
- Firth, I. M. (1977). Physics of the guitar at the Helmholtz and first top plate resonances. *Journal of Acoustical Society of America*, *61*(2), 588–593.
- Fletcher, N. H., & Rossing, T. D. (1998). The Physics of Musical Instruments. In *The Physics of Musical Instruments*. Springer. <https://doi.org/10.1007/978-0-387-21603-4>
- French, M., & Bissinger, G. (2001). Testing of acoustic stringed musical instruments—an introduction. *Experimental Techniques*, (February), 40–43. <https://doi.org/10.1111/j.1747-1567.2001.tb00007.x>
- French, M., & Hosler, D. (2001). the Mechanics of Guitars. *Experimental Techniques*, (June), 45–48. <https://doi.org/10.1111/j.1747-1567.2001.tb00025.x>
- Hansen, P. C. (2000). The L-Curve and its Use in the Numerical Treatment of Inverse Problems. *Computational Inverse Problems in Electrocardiology*, Ed. P. Johnston, *Advances in Computational Bioengineering*, *4*, 119–142. <https://doi.org/10.1.1.33.6040>
- Havimo, M. (2009). A literature-based study on the loss tangent of wood in connection with mechanical pulping. *Wood Science and Technology*, *43*(7–8), 627–642. <https://doi.org/10.1007/s00226-009-0271-4>
- Hess, D. (2013). Frequency Response Evaluation of Acoustic Guitar Modifications. *Savart Journal*, 1–8. Retrieved from <http://savartjournal.org/index.php/sj/article/view/19>
- Howard, D. M., & Angus, J. (2001). Acoustics and Psychoacoustics. *Focal Press, Oxford*.
- Hunt, D. G. (1999). A unified approach to creep of wood. *Proceedings of the Royal Society of London*.
- Hunt, D. G., & Balsan, E. (1996). Why old fiddles sound sweeter. *Nature*, *379*(6567), 681–681. <https://doi.org/10.1038/379681a0>
- Hutchins, C. M. (1998). A measurable effect of long-term playing on violin family instruments. *Catgut Acoustical Society Journal*, 38–44.
- Hutchins, C. M., Stetson, K. A., & Taylor, P. A. (1971). Clarification of “free plate tap tones” by holographic interferometry. *Catgut Acoustical Society Journal*, *16*(15).

- Hutchinson, J. M. (1995). Physical aging of polymers. *Prog Polym Sci*.
- Ibrahim, S. R., & Mikulcik, E. C. (1973). A time domain modal vibration test technique. *The Shock and Vibration Bulletin*, 43, 21–37.
- Inta, R., Smith, J., & Wolfe, J. (2005). Measurement of the effect on violins of ageing and playing. *Acoustics Australia*, 33(1), 25–29.
- Jansson, E. (1969). A comparison of acoustical measurements and hologram interferometry measurements of the vibrations of a guitar top plate. *Stl-Qpsr*, 10(2–3), 36–41.
- Jansson, E. V., Molin, N. E., & Sundin, H. (1970). On vibration modes of a violin top plate. A study by hologram interferometry. *Stl-Qpsr*, 11(2–3), 50–54.
- Juang, J.-N., & Pappa, R. S. (1985). An eigensystem realization algorithm for modal parameter identification and model reduction. *Journal of Guidance, Control, and Dynamics*, 8(5), 620–627. <https://doi.org/10.2514/3.20031>
- Kerschen, G., & Golinval, J.-C. (2000). Experimental Modal Analysis. *Vibration Fundamentals and Practice*.
- Knott, G. A. (1989). A modal analysis of the violin. *Finite Elements in Analysis and Design*, 5(3), 269–279.
- Obataya, E. (2017). Effects of natural and artificial ageing on the physical and acoustic properties of wood in musical instruments. *Journal of Cultural Heritage*, 27, 63–69. <https://doi.org/10.1016/j.culher.2016.02.011>
- Richardson, B. E., & Roberts, G. W. (1985). The adjustment of mode frequencies in guitars: A study by means of holographic interferometry and finite element analysis. *Proceedings of SMAC 83 (Publication of the Royal Swedish Academy of Music, No.46:2)*, 2, 285–302.
- Rossing, T. D. (2010). *The science of string instruments*. (Springer, Ed.), *The Science of String Instruments*. Springer. <https://doi.org/10.1007/978-1-4419-7110-4>
- Šali, S. (2002). Frequency response function of a guitar - a significant peak. *Catgut Acoustical Society*, 4(6), 1–13.
- Šali, S., & Kopač, J. (2000). Measuring a frequency response of a guitar. *Proceedings of the International Modal Analysis Conference - IMAC*, 2, 1375–1379.
- Šali, S., & Kopač, J. (2000). Measuring the quality of guitar tone. *Experimental Mechanics*, 40(3), 242–247. <https://doi.org/10.1007/BF02327495>

- Sobue, N., & Okayasu, S. (1992). Effects of Continuous Vibratin on Dynamic Viscoelasticity of Wood. *J. Soc. Mat. Sci., Japan*, 41(461), 164–169. Retrieved from papers2://publication/uuid/3CE61376-F03C-44E4-9BDE-9B314454D741
- Tapia, E. R. G. (2002). *Simulating a Classical Acoustic Guitar: Finite Element and Multiphysics Modelling*. KTH Royal Institute of Technology.
- Taub, H., & Schilling, D. L. (1986). *Principles of Communication Systems*. McGraw-Hill.
- Turner, R. (1997). Instant vintage: Can a vibration machine make a new guitar sound like an old guitar? *Acoustic Guitar Magazine*, 36–41.
- Van Karsen, D. (1997). Experimental Modal Analysis and Operating Deflection Shape of an Acoustic Guitar. *Proceedings of the 15th International Modal Analysis Conference*, 686–691.
- Van Overschee, P., & De Moor, B. (1996). *Subspace Identification for Linear Systems: Theory, Implementation, Applications*. Kluwer Academic Publishers.
- Virdung, S. (1511). *Musica getutscht und ausgezogen*. Basel.